Design of a Knee Exoskeleton for Gait Assistance

by

Vaibhav Jhawar

A Thesis Presented in Partial Fulfillment
of the Requirements for the Degree
Master of Science

Approved July 2018 by the
Graduate Supervisory Committee:

Wenlong Zhang, Chair
Thomas G. Sugar
Hyunglae Lee
Hamidreza Marvi

ARIZONA STATE UNIVERSITY

August 2018

ABSTRACT

The world population is aging. Age-related disorders such as stroke and spinal cord injury are increasing rapidly, and such patients often suffer from mobility impairment. Wearable robotic exoskeletons are developed that serve as rehabilitation devices for these patients. In this thesis, a knee exoskeleton design with higher torque output compared to the first version, is designed and fabricated.

A series elastic actuator is one of the many actuation mechanisms employed in exoskeletons. In this mechanism a torsion spring is used between the actuator and human joint. It serves as torque sensor and energy buffer, making it compact and safe.

A version of knee exoskeleton was developed using the SEA mechanism. It uses worm gear and spur gear combination to amplify the assistive torque generated from the DC motor. It weighs 1.57 kg and provides a maximum assistive torque of 11.26 N·m. It can be used as a rehabilitation device for patients affected with knee joint impairment.

A new version of exoskeleton design is proposed as an improvement over the first version. It consists of components such as brushless DC motor and planetary gear that are selected to meet the design requirements and biomechanical considerations. All the other components such as bevel gear and torsion spring are selected to be compatible with the exoskeleton. The frame of the exoskeleton is modeled in SolidWorks to be modular and easy to assemble. It is fabricated using sheet metal aluminum. It is designed to provide a maximum assistive torque of 23 N·m, two times over the present exoskeleton. A simple brace is 3D printed, making it easy to wear and use. It weighs 2.4 kg.

The exoskeleton is equipped with encoders that are used to measure spring deflection and motor angle. They act as sensors for precise control of the exoskeleton.

An impedance-based control is implemented using NI MyRIO, a FPGA based controller. The motor is controlled using a motor driver and powered using an external battery source. The bench tests and walking tests are presented. The new version of exoskeleton is compared with first version and state of the art devices.

To Mummy and Papa.

ACKNOWLEDGMENTS

I sincerely thank Dr. Wenlong Zhang for his encouragement and support throughout my thesis. Dr. Zhang is a great advisor and I am grateful to have worked with him. He has always been and will be an inspiration to me. He has given me a platform and all the resources and tools required not just to work on my project but also to help me grow as a person.

I also thank Dr. Thomas Sugar, Dr. Hyunglae Lee and Dr. Hamid Marvi for taking their time out of their busy schedule and their valuable feedback.

I would like to thank Pruthvi Tej Chinimilli for answering my endless questions and guiding me throughout, Zhi Qiao (George) for his help with discussing the design and for his ideas and implementation, Seyed Mostafa Rezayat for being a great labmate and sharing the journey with me. I also thank Iat Hou (Kevin) Fong for helping me begin the project, Shatadal Mishra and all the members of RISE lab, ASU for their help and support.

I thank Dr. Panagiotis Artemiadis, Dr. Yi Ren, and all my faculty for their invaluable lectures, Rhett Sweeney for helping me with my 3D CAD models and machining and Christine Quintero, my academic advisor for helping me throughout my master's program.

I would like to express my deepest love to my parents for their love, support, inspiration and encouragement. Many thanks to my sister, my grandparents, all my family members and my friends for their love and support.

TABLE OF CONTENTS

CHAPTER Page

LIST OF TABLES

LIST OF FIGURES

Figure Page

Chapter 1

INTRODUCTION

1.1 Background and motivation

810 million people were aged 60 and over across the world in 2012 and it is projected to double by 2050 according to United Nations Population Fund report (UNFPA (2012)) as the graphs show in Figure 1.1 and 1.2. In United States, the population aged 65 and over is projected to double from 43.1 million estimated in 2012 to 83.7 million in 2050 (Ortman *et al.* (2014)). Similar trend can be seen in many other countries (He *et al.* (2016)). The world population is aging. Aging leads to several diseases and disorders related to nervous system including stroke, spinal cord injury, multiple sclerosis, Alzheimer's disease, Parkinson's disease, arthritis and osteoporosis.

It impairs the mobility of the patients affected by these diseases and negatively

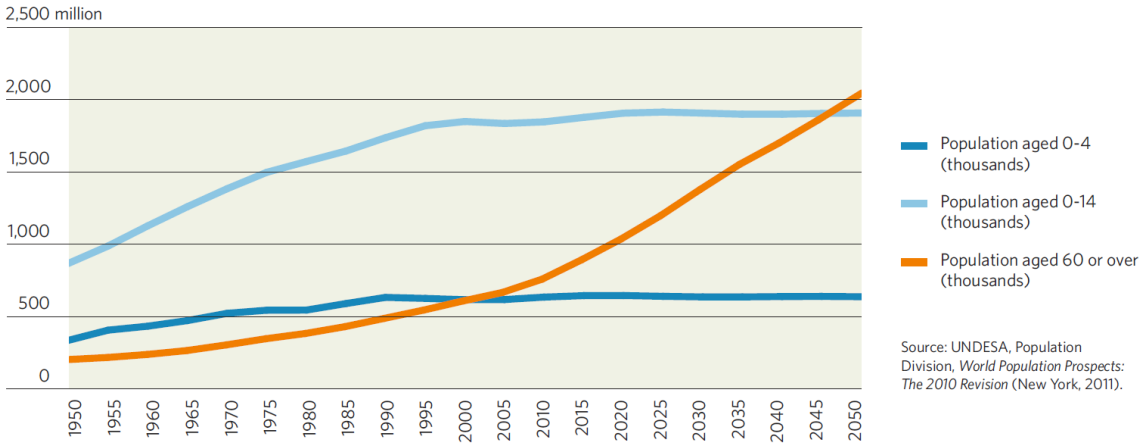

Figure 1.1: Trend of population aged 0-4, 0-14 and aged 60 or over: World, 1950 – 2050

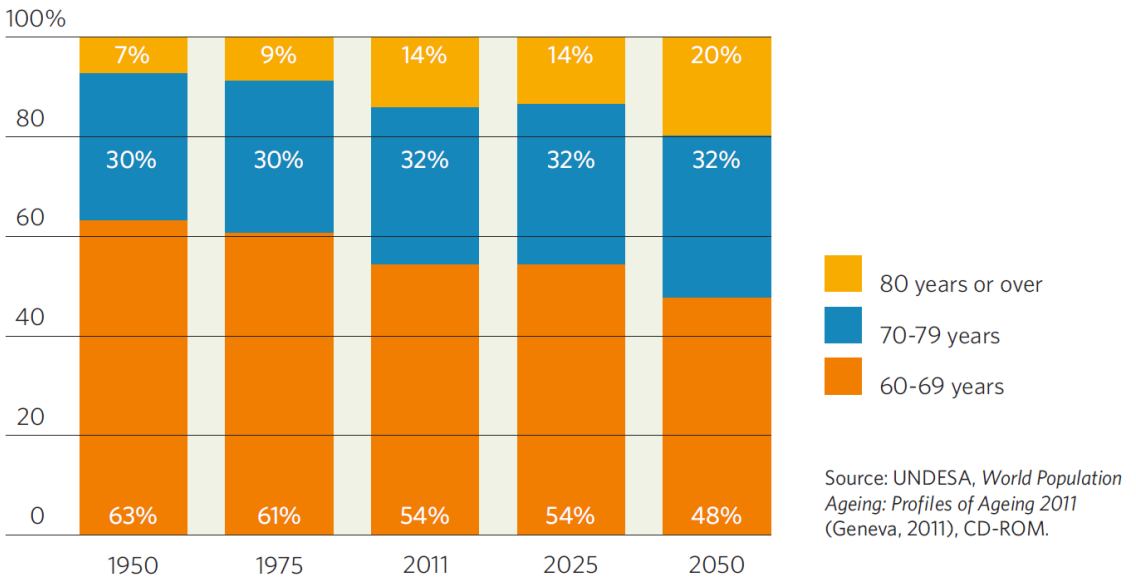

Figure 1.2: Distribution of population aged 60 years or over by broad age group: World, 1950 – 2050

affects their ability to live normally. It is sometimes temporary and partial, affecting one of the lower limbs. They have a chance to recover through rehabilitation training. With an increase in the number of patients, the demand for the rehabilitation also has increased over the years. However, most of rehabilitation training available is expensive and time consuming. It also requires intensive manual labor and supervision of experienced medical professionals which are limited to hospitals (Gage and Storey (2004)).

The need for personalized treatment in rehabilitation is increasing. Thanks to the advancements of robotic technology, it is now possible to develop compact and powerful wearable devices that could assist the patients with their daily routine tasks such as sitting, standing, walking. It could help them improve their health and aid in recovery in an efficient way.

1.2 State of the art

Exoskeletons are wearable devices that can assist patients with mobility impairment or augment the performance of the user. The history of the exoskeletons dates back to the 19th century and has grown ever since in terms of functionality and usability. There has been a steady growth of exoskeletons in the past two decades. Every aspect of mechanical and electrical engineering is explored in improving the design and functionality of the exoskeletons. Today, exoskeletons target different joints such as upper limbs and lower-extremity. They are also made passive and active and use a variety of different mechanisms and serve a variety of purposes such as rehabilitation, locomotion assistance, strength augmentation, hybrid and military use (Dollar and Herr (2008b); Herr (2009)). Earlier, the exoskeletons were primarily made for the purpose of strength augmentation. In recent years, with the improvement of technology and the demand for the personal rehabilitation, there has been a growth of exoskeletons as assistive devices for rehabilitation.

The very first exoskeleton in the recorded history is known to be of Nicholas Yagn's "Apparatus for facilitating walking, running, and jumping" for which he was granted a US patent in 1890 (Yagn (1890)). It used leaf springs to store and release energy to augment running as shown in Figure 1.3(a). It was a passive exoskeleton devoid of any electronics. It is not known to be ever built.

Forward to 1960, General Electric Research with researchers at Cornell University and financial support from the U.S. Office of Naval Research, constructed a full-body powered exoskeleton prototype 'Hardiman' (Mosher (1968); Gilbert and Callan (1968); Fick and Makinson (1971)) shown in Figure 1.3(b). It was a hydraulically powered machine weighing 680 kg. It was used to augment the strength of the user by 25 times. However, the technology available then made it very heavy with limited

(a) Yagn's walking aid (Yagn (1890))

(b) Hardiman (Fick and Makinson (1971))

(c) BLEEX (Kazerooni and Steger (2006))

(d) HAL-5 (Kawamoto *et al.* (2003))

Figure 1.3: Exoskeletons in the beginning: Yagn's walking aid, Hardiman, BLEEX and HAL.

functionality.

Some of the significant exoskeletons in the literature include BLEEX or the Berkeley Lower Extremity Exoskeleton developed at University of California, Berkeley. It is claimed as the first load-bearing and energetically autonomous exoskeleton (Kazerooni and Steger (2006)) shown in Figure 1.3(c). It features three degrees of freedom (DOF) at the hip, one at the knee, and three at the ankle. It is actuated with linear hydraulic actuators at four joints, two at hip, one at knee and one at ankle. BLEEX can support a load of up to 75 kg while walking at 0.9 m/s and can walk at speeds of up to 1.3 m/s without the load.

HAL-5 is another full body exoskeleton. It is developed by Prof. Yoshikuyi Sankai and his team at the University of Tsukuba, Japan (Kawamoto and Sankai (2002); Kawamoto *et al.* (2003)). It is targeted for both performance augmentation and rehabilitative purposes and weighs 10 kg, shown in Figure 1.3(d). It uses nerve signals sent from brain to the muscles to control the movement of the exoskeleton.

Unlike full-body exoskeletons which also support or assist upper limbs, lower-

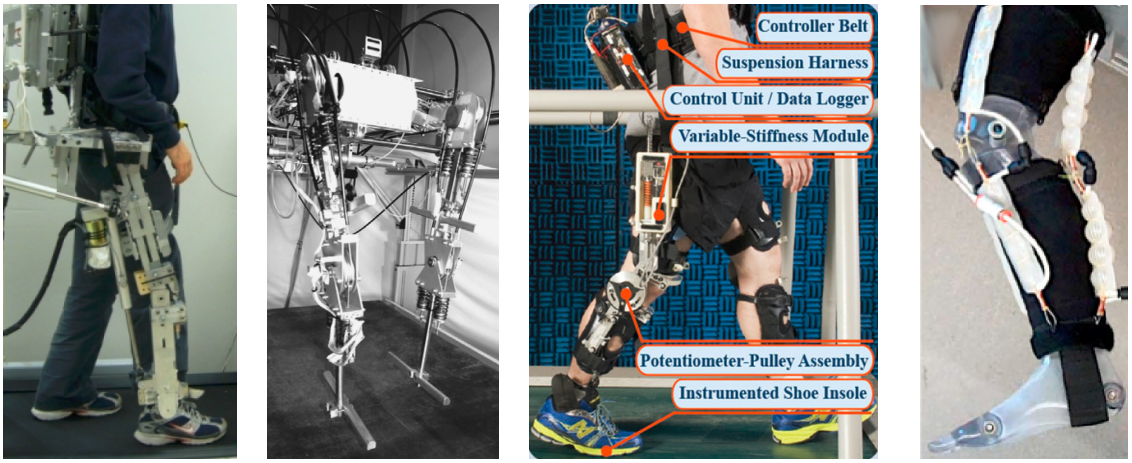

(a) ALEX (Banala *et al.* (2009))

(b) LOPES (Veneman *et al.* (2007))

(c) Spring exoskeleton (Shamaei *et al.* (2015))

(d) Soft exoskeleton (Park *et al.* (2014))

Figure 1.4: Knee exoskeleton designs: ALEX, LOPES, parallel Spring Exoskeleton and soft exoskeleton.

extremity exoskeletons are used to target and assist joints on the lower limb such as hip, knee and ankle. These are used in rehabilitation to help patients who are affected with the lower limb mobility impairment. In some cases, one or more joints are passive and other joints are actively assisted. Some of the lower-extremity exoskeletons and their details are mentioned below.

ALEX (Active Leg EXoskeleton) is a powered leg orthosis with linear actuators at the hip and knee joints (Banala *et al.* (2009)) shown in Figure 1.4(a). It implements a force-field controller which can apply suitable forces on the leg to help it move on a desired trajectory.

LOPES (LOwer-extremity Powered ExoSkeleton) (Veneman *et al.* (2007)) shown in Figure 1.4(b) is a rehabilitation device with three actuated rotational joints: two at the hip and one at the knee. The joints are actuated with Bowden-cable driven series elastic actuators.

Human knee approximately behaves as a linear torsion spring and the parameters of the spring can be identified as shown by (Shamaei and Dollar (2011)). An

(a) Ekso GT (Pransky (2014))

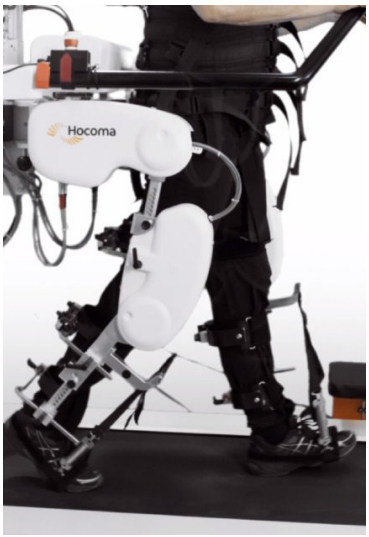

(b) Lokomat (Colombo *et al.* (2000))

(c) FORTIS (Lockheed Martin (2018))

Figure 1.5: Commercially available exoskeletons: Ekso GT, Lokomat and FORTIS.

exoskeleton with an external torsion spring in parallel to the knee joint can be used to reduce the contribution of knee joint in stance phase as shown by (Shamaei *et al.* (2015)) in Figure 1.4(c).

A safer and lightweight alternative to rigid exoskeletons are soft suits that use soft robotics as wearable assistance (Polygerinos *et al.* (2017)). These use pneumatics or hydraulics to pump fluid to soft fabric to inflate or deflate, thus enabling the actuation. An example of soft exoskeleton using elastomeric artificial muscle actuators (Park *et al.* (2014)) is shown in Figure 1.4(d). There is however a limitation with power, accuracy and latency with the soft actuation.

Many exoskeletons are developed commercially both for strength augmentation and clinical rehabilitation. Examples of such exoskeletons include Ekso GT exoskeleton, a wearable exoskeleton suit designed for the assistance and rehabilitation of patients by Ekso Bionics (Pransky (2014)) shown in Figure 1.5(a). Lokomat, a treadmill-based body weight support device developed by Hocoma (Switzerland) (Colombo

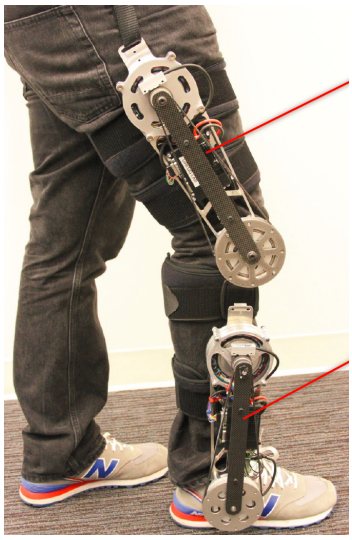

(a) Torque dense exoskeleton (Zhu *et al.* (2017))

(b) AKROD (Weinberg *et al.* (2007))

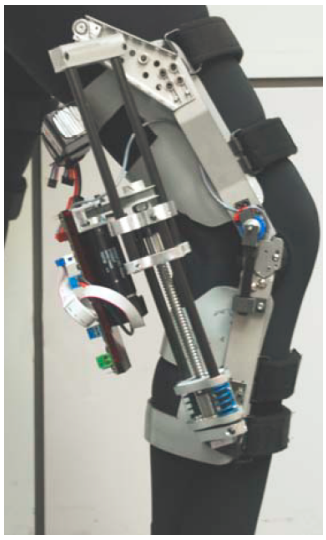

(c) Running assistance device (Dollar and Herr (2008a))

Figure 1.6: Exoskeleton designs: Torque dense exoskeleton, AKROD and running assistance device.

et al. (2000)) shown in Figure 1.5(b) and Lockheed Martin developed FORTIS (Lockheed Martin (2018)) for industrial use to augment the strength of the worker shown in Figure 1.5(c).

Knee exoskeletons are a subset of lower-extremity exoskeletons which target specifically the knee joint. They usually have one degree-of-freedom which assist the patients in the sagittal plane. Some of the knee-exoskeleton designs are detailed below.

A torque dense and backdrivable knee-ankle exoskeleton is presented by (Zhu *et al.* (2017)) shown in Figure 1.6(a). It uses a high torque motor and planetary gear with timing belt to achieve a continuous torque of 30 N·m. It weighs 4.88 kg in total. Active Knee Rehabilitation Orthotic Device (AKROD) shown in Figure 1.6(b) is designed to train stroke patients (Weinberg *et al.* (2007)). The knee brace provides variable damping controlled in ways that foster motor recovery in stroke patients. In this, a resistive, variable damper, electrorheological fluid (ERF) based component is used to facilitate knee flexion during stance by providing resistance to knee buckling.

(a) RoboKnee (Pratt *et al.* (2004))

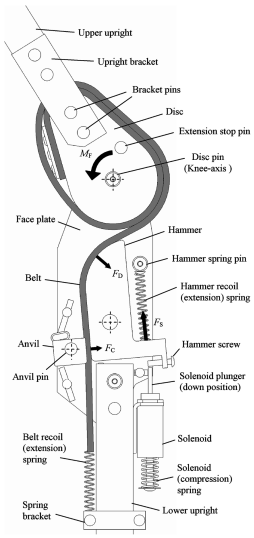

(b) Exoskeleton using solenoid (Yakimovich *et al.* (2006))

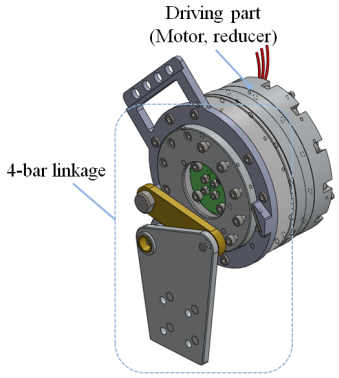

(c) Exoskeleton using fourbar linkage (Kim *et al.* (2015))

Figure 1.7: Knee exoskeleton designs: RoboKnee, exoskeleton using solenoid and exoskeleton using fourbar linkage.

In (Dollar and Herr (2008a)), a device is proposed which consists of a knee brace in which a motorized mechanism actively places and removes a spring in parallel with the knee joint to assist running as shown in Figure 1.6(c).

RoboKnee is a one degree of freedom exoskeleton shown in Figure 1.7(a) where user intent is determined through the knee joint angle and ground reaction forces and it uses series elastic actuators (Pratt *et al.* (2004)). To enable a more natural gait, in (Yakimovich *et al.* (2006)), a friction-based belt-clamping mechanism is employed in electromechanical stance-control knee-ankle-foot orthosis (SCKAFO) as shown in Figure 1.7(b). A modular knee exoskeleton system that supports the knee joints of hemiplegic patients is presented in (Kim *et al.* (2015)). The device is designed to realize the polycentric motion of real human knees using a fourbar linkage as shown in Figure 1.7(c).

Work is also being done on varying the stiffness of the series elastic actuator. In (Bolivar *et al.* (2016)) the actuator uses a dielectric elastomer as the series elastic

element so that the stiffness of the actuator can be electrically modulated. Another method to store energy and improve the performance of series elastic actuator is to have a leaf spring in parallel to the series elastic actuator (Zhu *et al.* (2014)).

Many different transmission mechanisms are used to drive the exoskeletons such as cable driven actuators (Veneman *et al.* (2007); Celebi *et al.* (2013)) which uses Bowden-cable that can be connected to an off-site motor to actuate the joints, series elastic actuators (Kong *et al.* (2012); Kim and Bae (2017)) which uses elastic element in series with actuator and joint, variable stiffness actuators (Grosu *et al.* (2017); Wolf *et al.* (2016)) in which the stiffness and impedance are varied by using additional motors and springs and soft actuators (Park *et al.* (2014); Sridar *et al.* (2018)) that uses soft inflatable materials as actuators. Each of these actuators has their own advantages and limitations. The series elastic actuator, its characteristics and benefits are studied in the next subsection.

1.3 Series elastic actuator

Series elastic actuator (SEA) is a mechanism which has an elastic element between the actuator and the load (Pratt and Williamson (1995); Robinson (2000)). The elastic element could be a torsion spring (Kong *et al.* (2012)) or fiberglass beam spring (Shepherd and Rouse (2017)). An example is torsion spring between geared motor and lever arm connecting the human knee joint. A block diagram of SEA is shown in Figure 1.8.

The spring enables slight relative motion between motor and human which makes it unique and has some advantages over the stiffer mechanisms.

The spring in the SEA can also be used as a torque sensor. By measuring the deflection on the two ends of the spring which are connected to motor and end-effector, and knowing the spring constant, the torque can be determined. The SEA acts like

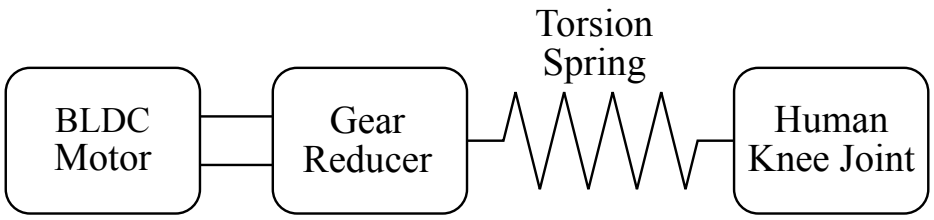

Figure 1.8: Block diagram of a series elastic actuator.

a shock absorber and has low output impedance. Therefore, any unintended motion from the human side is not transferred to the motor and it prevents any unexpected high torque from the motor to be transferred to the human side. It can also store and release energy at the desired instant.

The characteristics of series elastic actuator include low output impedance, impact resistance ability, high force control precision and stability and capability of energy storage to improve the efficiency of the system. These characteristics make the SEA safe and applicable for the exoskeletons used in rehabilitation.

1.4 Objective and scope

To improve the quality of life of the patient, particularly to aid the rehabilitation of lower limb mobility, a knee exoskeleton is to be designed and fabricated. A version of knee exoskeleton was designed and fabricated in RISE lab, the details of which are presented in Chapter 2. It has several limitations. It is difficult to wear and to use it for a long period of time. It also has low assistive torque for its weight. Therefore, the torque to weight ratio is also low. It is difficult to assemble and difficult to customize.

Therefore, to overcome the limitations in this version of exoskeleton, the following objectives are stated for this thesis work. A new knee exoskeleton for gait assistance

is to be designed, fabricated and assembled. It should use series elastic actuator as the actuation mechanism. It should be compact and lightweight. It should have high assistive torque and high torque to weight ratio. It should be safe and easy to wear and use.

1.5 Chapter summary and thesis outline

In this chapter, the problem of aging and age-related disorders is introduced along with the need for wearable assistive exoskeletons. Various types of exoskeletons including lower-extremity and knee exoskeletons are presented and studied. The series elastic actuator, its characteristics and advantages are studied in detail. Finally, the objective of the thesis is stated.

The following chapters of this thesis are organized as follows. In chapter 2, the design of the first version of exoskeleton is studied. The motivation for a new version of exoskeleton is presented. The design of second version of exoskeleton is explored in detail including design requirements based on the human gait characteristics and component selection based on component specifications. The details of the CAD model and assembly of the exoskeleton is also presented. Chapter 3 deals with control and testing of the exoskeleton in detail. In chapter 4, a comparison of the two versions of the exoskeletons and the comparison of the new exoskeleton with the state of the art is presented and discussion is done. Finally, conclusion is done and future work is presented in chapter 5.

Chapter 2

DESIGN OF THE KNEE EXOSKELETON

2.1 Exoskeleton - version 1

Inspired by the Kong's cRSEA (compact rotary series elastic actuator) (Kong *et al.* (2012)) designed at University of California, Berkeley that uses series elastic actuator, an exoskeleton was designed and fabricated in RISE lab, ASU by Iat Hou Fong. It is an assistive device used for gait rehabilitation. It uses a worm gear and spur gear combination to amplify the assistive torque generated by a DC motor. The CAD model of the exoskeleton is shown in Figure 2.1.

Maxon RE 40, a 150W DC Motor is used to power the exoskeleton. This motor was selected so that with amplification it can provide a fraction of maximum knee

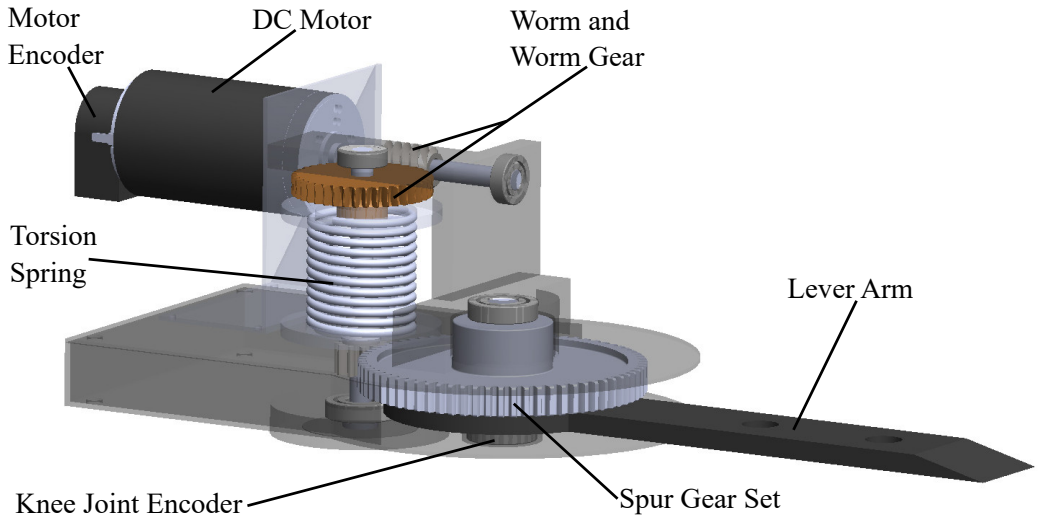

Figure 2.1: CAD model of exoskeleton version 1.

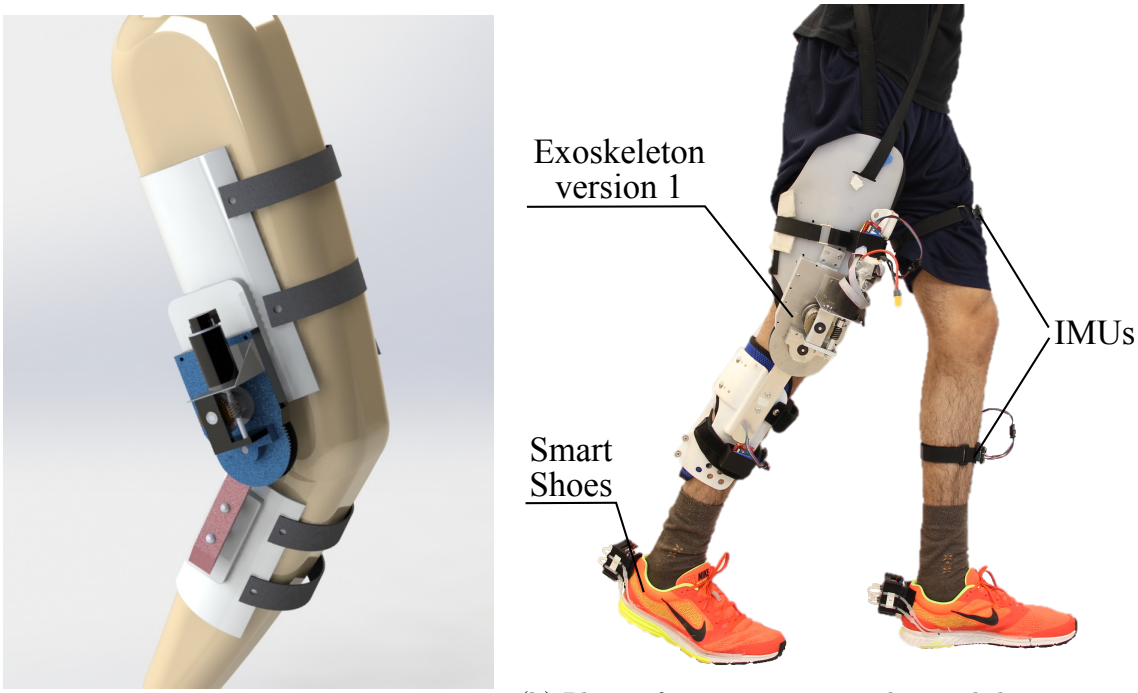

(a) Illustration of the exoskeleton version 1.

(b) Photo of a person wearing the exoskeleton version 1 with smart shoes and IMUs.

Figure 2.2: An illustration and photograph of exoskeleton version 1.

moment as the assistive torque and cover entire knee angular velocity range in gait cycle. It has a nominal torque of 0.177 N·mm and nominal speed of 6940 rpm. The worm and worm gear has a reduction ratio of 10:1. The spur gear has a reduction ratio of 6.36:1. With the combined reduction ratio of 63.6:1, the end-effector can reach a maximum angular velocity of 120 rpm (rotations per minute) and the motor can provide a maximum continuous assistive torque of 11.26 N·m.

Two incremental optical rotary encoders are used in this exoskeleton. One encoder is placed on the motor and it is used to measure motor angle. The motor can be controlled by receiving feedback from the motor encoder. The other encoder is placed on the spur gear and it is used to measure the human knee angle. Human knee angular velocity can be calculated from the human knee angle. In combination, these encoders are used to control the exoskeleton.

Table 2.1: Design specification of the components of exoskeleton version 1.

Component	Specification	Value
Torsion spring	Spring constant	6.59 N·mm/deg
	Max angular deflection	317 degrees
Worm gear	Gear ratio	10:1
	Pressure angle	25 degrees
	Lead angle	18.26 degrees
Spur gear	Gear ratio	6.36:1
	Pressure angle	14.5 degrees
Encoders	Resolution	2000 counts/turn

The exoskeleton is also equipped with a torsion spring between the worm gear and spur gear. It is an elastic element which serves as a torque sensor, by enabling the relative motion between motor and end-effector. It also provides an energy buffer to prevent injuries to the user from unexpected high motor torques. The torsion spring has a spring constant of 6.590 N-mm/deg and maximum deflection of 317 degrees. It can withstand a maximum torque of 2.033 N·m which is greater than the maximum torque from the motor amplified by the worm gear.

The specifications of the components used in the exoskeleton are given in Table 2.1. The weight of the KAD including the components and frame is 1.57 kg. The weight of the brace is 0.83 kg, making it heavy with a total weight of 2.4 kg. A photo of a person wearing the exoskeleton along with smart shoes and IMUs is shown in Figure 2.2(b). Smart shoes use silicone tubes that are wound into air bladders and connected to barometric sensors. There are four sensors which measure the ground contact forces (GCF) on the heel, first metatarsal joint (Meta 1), fourth metatarsal joint (Meta 4) and toe (Zhang *et al.* (2016); Chinimilli *et al.* (2016)). Inertial measurement units (IMU) are devices that uses accelerometers and gyroscopes to measure the angular rate and calculate the angle. In combination, these devices can be used to estimate

the gait phases, gait activities and human intention. These can be incorporated in the control algorithm to improve the performance of the exoskeleton. The details of the control algorithm are mentioned in Chapter 3.

2.2 Motivation for a new exoskeleton

The first version of the exoskeleton is compact and light. Yet, there is scope for improvement and flaws to overcome. One of the problems that can be immediately observed is that it is difficult to wear and to use it for a long period of time. Rehabilitation training sessions often require prolonged use of the assistive device. Part of the problem is due to the bulky brace used to mount the exoskeleton on the body. Therefore, a better bracing support needs to be designed that is easier to wear and use. It must be compact and lightweight.

This exoskeleton also has low assistive torque for its weight. Higher assistive torque could help the patients recover quickly. However, increasing the torque output generally requires bigger and heavier motor. Therefore, the weight of the exoskeleton should be considered when designing the exoskeleton. For this, torque to weight ratio should be as high as possible.

Also, there is greater chance of misalignment in the transmission because of changes in the direction of the motion. The complexity of the design also makes the exoskeleton difficult to assemble and difficult to customize. Some of these problems are easy to overcome by designing a better frame and transmission mechanism, while the problem of torque and weight could be addressed using better components.

For the remainder of the thesis, the two exoskeletons are referred as exoskeleton version 1 and exoskeleton version 2 for the purpose of readability and clarity.

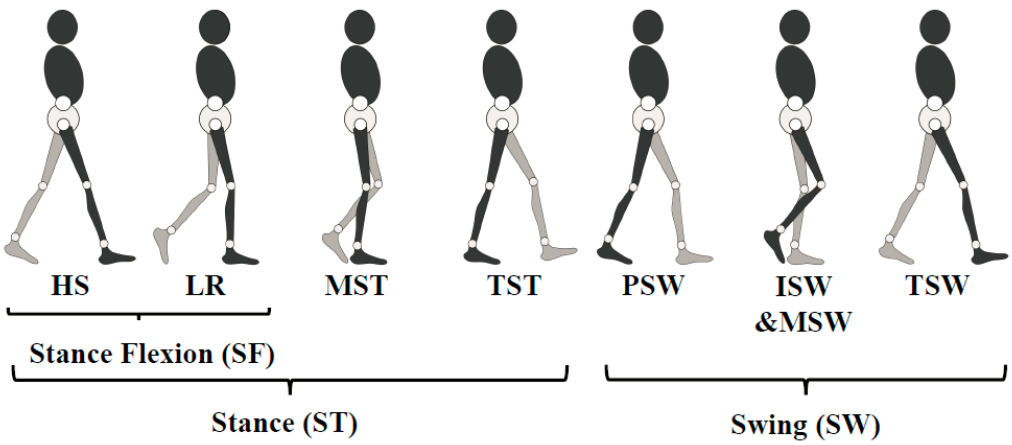

Figure 2.3: The gait cycle of human walking. HS - heel strike, LR - loading response, MST - mid stance, TST - terminal stance, PSW - pre-swing, ISW - initial swing, MSW - mid swing, and TSW - terminal swing (Chinimilli *et al.* (2018)).

2.3 Exoskeleton - version 2

2.3.1 Design requirements and consideration

The objective as discussed in the Chapter 1, the exoskeleton version 2 should in general have higher torque output, be compact, lightweight, easy to wear and use. From the mechanical design perspective, it should be easy to manufacture, easy to assemble and disassemble, and have scope for future modifications. It should not have any alignment issues and should be reliable over time.

Biomechanical factors are to be considered as primary design requirement. These include degrees-of-freedom (DOFs), range-of-motion (ROM), joint torque requirements, joint rotational velocity, and joint angular bandwidth (Cenciarini and Dollar (2011)). In this thesis, joint torque, joint rotational velocity and ROM are considered as the design requirements for the exoskeleton version 2.

To define the torque requirements, it is important to first understand and study the human knee joint characteristics and gait patterns during walking. An experiment was set up in the motion capture laboratory equipped with 12 high-speed infrared

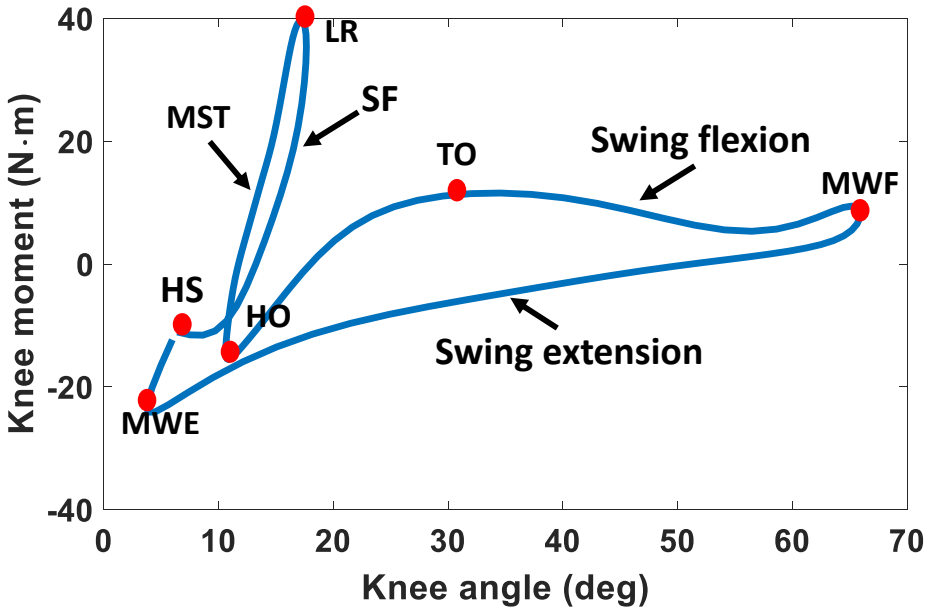

Figure 2.4: Knee moment v.s knee angular velocity in a gait cycle during level walking (Chinimilli *et al.* (2018)).

cameras (Vicon Motion Systems Ltd.,) and instrumented treadmill (Bertec Corporation). Markers were put on the lower body and a level walking trial with speed of the treadmill set to 0.8 m/s was conducted. The knee moment is calculated by the plug-in gait Vicon software which takes ground reaction forces from instrumented treadmill and marker's position as inputs.

Figure 2.3 shows the gait cycle of human walking and Figure 2.4 shows the plot of knee joint moment v.s knee angular velocity in a gait cycle during level walking (Chinimilli *et al.* (2018)). The average human knee angle ranges from 0 – 67 degrees. The knee angle is measured as the angle between the thigh and leg; +ve for flexion, -ve for extension. The knee moment ranges from -25 – 40 N·m and the knee angular velocity ranges from -350 – 300 deg/s (-58.33 – 50 rpm) (Winter (1991)).

As this exoskeleton is designed to use for rehabilitation, a fraction of maximum knee moment should be considered as the maximum output torque of the exoskeleton.

This can be later controlled using different algorithms that uses gait parameters. A maximum output torque of about 20 N·m can be considered as the maximum torque output for the exoskeleton version 2 design which is about half of the maximum knee moment. It is also double compared to the maximum torque of the exoskeleton version 1.

The maximum speed (angular velocity) of this exoskeleton should be such that it should cover entire gait cycle and leave enough margin for any deviations. The maximum speed of the knee joint is 58.3 rpm. Considering a factor of 1.5, about 90 rpm could be the maximum speed of the exoskeleton. The total weight of this exoskeleton could be capped at 3 kg, thus bringing the torque to weight ratio to 7.7 N·m/kg from 4.7 N·m/kg.

To make the selection process easier, another unit called converted power is defined. It is the product of the maximum required output torque in N·m and the maximum required speed in rpm. In this case the number is 1800, obtained by multiplying 20 N·m $\times$ 90 rpm.

One of the important design factors is the safety of the patient/user, which should be an important consideration in every stage of the design. In a series elastic actuator, the spring acts as energy buffer and prevents the human from unexpected high torque from the motor making the exoskeleton safe. Other safety mechanisms such as emergency stop, software and hardware limits could be added to the exoskeleton design.

The exoskeleton version 2 consists of 6 major components 1) actuator 2) amplifier 3) elastic component 4) frame 5) encoders and 6) electronic accessories (controller, motor driver and battery). These components are selected based on the above design considerations. The selection process is elaborated in the next sections.

2.3.2 BLDC motor

There are many actuation techniques such as pneumatic, hydraulic and electric motor. In this design, a DC motor is selected as it is compact for the same power output compared to other actuators.

The selection of the motor is done in the following way. First, an extensive list of all the potential motors that could satisfy the design requirements is made. The properties and specifications of the motors are also collected. It includes their size, weight, electrical power, voltage, torque, speed, cost, and market availability. Table 2.2 presents the list of motors with the specifications.

The next step is to convert these specifications to the required parameters such as torque to weight ratio, power to weight, converted torque, converted rpm, converted power (torque $\times$ rpm) as done in Table 2.3. Since the required torque is 20 N·m, the torque of the motor is multiplied by a factor to get to 20 N·m, this is the converted torque. Converted rpm is then the rpm of the motor multiplied by the factor obtained from the converted torque. Converted power is the product of converted torque and converted rpm. This is a user defined unit and its value should be greater than 1800 as discussed in the beginning of the section. The multiplication factor from the selected motor will be used in the selection of the gear reducer.

Although, brushed motors are inexpensive and simple to control, brushless motors offer many advantages over the brushed motors. They rank high in efficiency, offer higher power output for the same given size. They also dissipate heat better than the brushed motor. Hence, priority is given for the brushless motor over brushed motors in the selection process. Similarly, less weight, small size, high power, high torque and high speed are also prioritized.

Based on the above selection criteria, among all the motors, motor number 1 sat-

Table 2.2: Extensive list of all the motors that satisfies the design requirements.

	Company	Motor	Brush/ Brushless	Voltage (V)	Power (W)	Torque (N·mm)	Speed (rpm)	Weight (g)	size (mm)	Cost ($)
1	Maxon	EC-i 52-574741	Brushless	24	180	434	4220	820	52	396.38
2	Maxon	EC 45-136207	Brushless	24	250	331	4300	1100	45	792.38
3	Maxon	EC 45-136210	Brushless	24	250	311	7970	1100	45	792.38
4	Maxon	EC 45-136198	Brushless	24	150	183	4840	850	45	694.25
5	Maxon	EC 45-136204	Brushless	24	150	169	9290	850	45	694.25
6	Maxon	RE 40-148867	Brushed	24	150	177	6940	480	40	478.13
7	Maxon	RE 65-388985	Brushed	24	250	484	3810	2100	65	993.63
8	Maxon	RE 65-353295	Brushed	24	250	697	3810	2100	65	993.63
9	Maxon	RE 65-388985	Brushed	24	250	484	3810	2100	65	993.63
10	Maxon	RE 50-370354	Brushed	24	200	405	5680	1100	50	588.5
11	Maxon	RE 50-389089	Brushed	24	200	385	5690	1100	50	588.5
12	Maxon	BN34-25AF-01	Brushless	24	361	423	8130	1020	86.36	∼900
13	Maxon	BN28-21AF-01	Brushless	24	210.3	218	9170	653.2	71.12	∼900
14	Maxon	BN28-29AF-01	Brushless	24	262.4	282	8870	994	71.12	∼900
15	Moog	BN28-36AF-01	Brushless	24	296.2	480	5890	1363	71.12	∼900
16	Moog	BN28-44AF-01	Brushless	24	289.5	593	4660	1732.4	71.12	∼900
17	Moog	BN34HS-25AF-01	Brushless	24	396	240	14011	1072	86.36	∼900
18	Moog	BN34HS-35AF-01	Brushless	24	478	550	7100	1846	86.36	∼900
19	BEI Kimco	DIH23-30-007A	Brushless	8.4	349.44	282	4000	793.78	57.15	
20	BEI Kimco	DIH23-25-001A	Brushless	28.7	165.03	176		510.3	57.15	
21	Oriental	BLV620K20S	Brushless	24	200	11700	5∼200	600	110	948
22	Oriental	BLV620K10S	Brushless	24	200	5900	10∼400	600	110	948
23	Oriental	BLV620K30S	Brushless	24	200	16800	3.3∼133	600	110	960
24	Oriental	BLV620K50S	Brushless	24	200	28800	20∼80	600	110	960
25	Allied Motion	CM-2600	Brushless	24	22.3	200	1125		66.3	

Table 2.3: Extensive list of all the motors that satisfies the design requirements continued.

	Torque to Wt. Ratio	Power to Wt. Ratio	Converted Torque	Converted rpm	Converted Power (Torque×rpm)
1	0.5293	2.23	20.398	89.78	1831.48
2	0.3009	1.29	20.522	69.35	1423.3
3	0.2827	2.25	20.526	120.76	2478.67
4	0.2153	1.04	20.13	44	885.72
5	0.1988	1.85	20.28	77.42	1570.01
6	0.3688	2.56	8.319	147.66	1228.38
7	0.2305	0.88	22.748	81.06	1844.04
8	0.3319	1.26	32.759	81.06	2655.57
9	0.2305	0.88	22.748	81.06	1844.04
10	0.3682	2.09	19.035	120.85	2300.4
11	0.3500	1.99	18.095	121.06	2190.65
12	0.4147	3.37	20.304	169.38	3438.99
13	0.3337	3.06	20.056	99.67	1999.06
14	0.2837	2.52	20.022	124.93	2501.34
15	0.3522	2.07	20.16	140.24	2827.2
16	0.3423	1.6	20.162	137.06	2763.38
17	0.2239	3.14	20.16	166.8	3362.64
18	0.2979	2.12	20.35	191.89	3905

isfies all the requirements and ranks higher. It is Maxon EC-i 52 ϕ52 mm, brushless, 180 W, with Hall sensors, Part number 574741. The image of motor is shown in Figure 2.5 and the complete specifications of this motor are presented in Table 2.4, which are acquired from the Maxon Motors' website.

2.3.3 Planetary gear

The torque obtained from the motor needs to be amplified to the required amount. Many different types of amplification techniques can be used for this purpose, such as gears, lead screw, ball screw, belt drive, etc.

Lead screw and ball screw convert the rotary motion of the motor to linear motion. They take up lot of space which is not desired. The reduction ratio of belt drive is

Table 2.4: Specification of Maxon EC-i 52 BLDC motor.

Values at nominal voltage	
Nominal voltage	24 V
No load speed	4720 rpm
No load current	716 mA
Nominal speed	4220 rpm
Nominal torque (max. continuous torque)	434 N·mm
Nominal current (max. continuous current)	8.96 A
Stall torque	12200 N·mm
Stall current	253 A
Max. efficiency	90 %
Characteristics	
Terminal resistance	0.0948 Ω
Terminal inductance	0.123 mH
Torque constant	48.1 N·mm/A
Speed constant	198 rpm/V
Speed / torque gradient	0.391 rpm/N·mm
Mechanical time constant	0.696 ms
Rotor inertia	170 g cm^2
Thermal data	
Thermal resistance housing-ambient	4.32 K/W
Thermal resistance winding-housing	0.63 K/W
Thermal time constant winding	19.9 s
Thermal time constant motor	1780 s
Ambient temperature	−40 °C to 100 °C
Max. winding temperature	155 °C
Mechanical data	
Max. speed	6000 rpm
Axial play	0 - 0.14 mm
Max. axial load (dynamic)	12 N
Max. force for press fits (static)	150 N
(static, shaft supported)	6000 N
Max. radial load	110 N, 5 mm from flange
Other specifications	
Number of pole pairs	8
Number of phases	3
Number of autoclave cycles	0
Product	
Weight	820 g

Figure 2.5: Maxon EC-i 52 BLDC Motor.

limited, and it requires preloading and frequent maintenance. In this design, gear transmission is used for its compactness, strength and reliability.

Again, there are many different types of gears to choose from such as spur gear, helical gear, bevel gear, hypoid gear, worm and worm gear, planetary gear and harmonic drive. All these types of gear mechanisms are used in literature and they have their own benefits and limitations.

For high torque amplification and high-speed reduction, the following types of gears are suited, hypoid gear, planetary gear and harmonic drive. Hypoid gear suffers from wear and tear and although harmonic drives are compact, they have low power and strength. Planetary gear is chosen in this design for its accuracy, strength and reliability.

Based on the compatibility and the reduction factor to amplify the torque, the following planetary gear is selected. Maxon Planetary Gearhead GP 52 C ϕ52 mm, 4 – 30 N·m, Ceramic Version, Part number 223090. It has a reduction ratio of 53:1 which converts the maximum motor torque to 23 N·m, which is higher than the maximum required torque. The complete specifications of this planetary gear are presented in Table 2.5, which are acquired from the Maxon Motors' website. The image of the planetary gear is shown in Figure 2.6.

Table 2.5: Specification of the Maxon Planetary Gearhead GP 52 C.

General information	
Gearhead type	GP
Outer diameter	52 mm
Version Ceramic	version
Gearhead Data	
Reduction	53 : 1
Absolute reduction	637/12
Max. motor shaft diameter	10 mm
Number of stages	3
Max. continuous torque	30 N·m
Max. intermittent torque	45 N·m
Direction of rotation, drive to output	=
Max. efficiency	75 %
Average backlash no load	1°
Mass inertia	$17.2\,\mathrm{g\,cm^2}$
Gearhead length (L1)	78.5 mm
Max. transmittable power (continuous)	360 W
Max. transmittable power (intermittent)	530 W
Technical Data	
Radial play max.	0.06 mm, 12 mm from flange
Axial play	0 - 0.3 mm
Max. radial load	900 N, 12 mm from flange
Max. axial load (dynamic)	200 N
Max. force for press fits	500 N
Max. continuous input speed	6000 rpm
Max. intermittent input speed	6000 rpm
Recommended temperature range	−50 °C to 80 °C
Extended temperature range	−40 °C to 100 °C
Number of autoclave cycles	0
Product	
Weight	770 g

Figure 2.6: Maxon Planetary Gearhead GP 52 C.

Table 2.6: Specification of the spiral bevel gear.

Specification	Value
Part Number	21075S0111
Nominal Torque	45 N·mm
Max Torque	68 N·mm
Max Speed	6500 rpm
Gear Ratio	1:1
No. of teeth	26
Max. diameter	45 mm

2.3.4 Bevel gear

The motor and planetary gear if connected directly to the knee joint will increase the lateral length in the coronal plane, which is against the design requirement defined earlier. Hence, to change the direction of torque transmission and retain the reduction ratio, a bevel gear with 1:1 ratio is used.

The requirements for bevel gear are, it should be tough and its surface should be hard to be able to withstand the high torque and mechanical shock. It must also be small in size, so that the exoskeleton remains compact. Considering this, the following spiral bevel gear is chosen. It is shown in Figure 2.7 and its properties are detailed in Table 2.6.

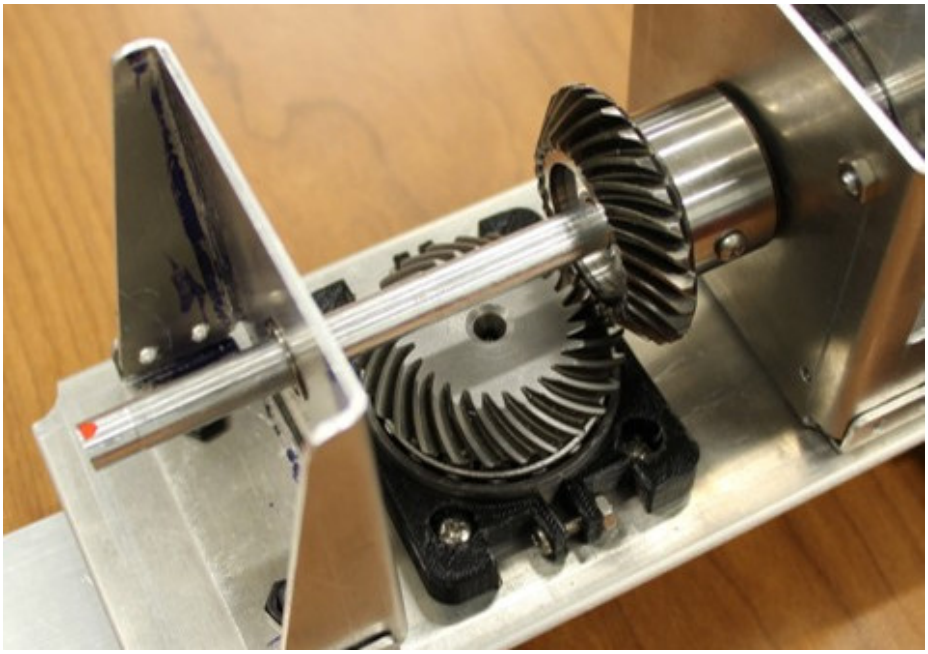

Figure 2.7: Spiral bevel gear with 1:1 gear ratio.

2.3.5 Spring

The torsion spring plays a very important role in the series elastic actuation as discussed in Chapter 1. In this exoskeleton, it connects the planetary gear and the bevel gear in series.

The torsion spring should be able to withstand the amplified torque from the planetary gear and allow a maximum deflection between the planetary gear

and the bevel gear/ knee joint by a factor of the knee joint motion. Hence, the maximum torque and maximum deflection serves as the criteria for selection of spring.

The spring used can be varied in length and diameter if required as detailed later in the frame design. Two different types of springs are shown in Figure 2.8.

Unlike the previous design, where encoders are placed on the beginning and end of the mechanism, the encoders in the new design are placed immediately after the spring. This allows for accurate measurement of the spring deflection, and hence

Figure 2.8: Different torsion springs that can be used in the exoskeleton version 2.

better estimation of the assistive torque.

The specifications of the encoders used in the exoskeleton are mentioned in the next section.

2.3.6 Encoders

Encoders are used to measure the angle by converting the angular position of the shaft to electrical signal. There are many types of encoders such as incremental, absolute, optical, conductive and magnetic. These encoders act as sensors in this exoskeleton.

Three encoders are used in this exoskeleton. One of the encoders is attached to the motor and it is used solely to measure motor angle and to control the motor. Other two encoders are used to measure the angular deflection of the spring. In combination, these encoders are used to precisely control the exoskeleton.

Only two of the three encoders may be used depending upon the design of the control algorithm and the controller used. Having a redundant encoder allows for this flexibility.

The Motor encoder used in the exoskeleton is 'Encoder HEDL 5540, 500 CPT, 3 Channels, with Line Driver RS 422' from Maxon Motors, Part number 110518. It is

Table 2.7: Specification of the motor encoder.

General information	
Counts per turn	500
Number of channels	3
Line Driver	DS26LS31
Max. mechanical speed	12000 rpm
Shaft diameter	8 mm
Technical Data	
Supply voltage Vcc	5.0V 10.0%
Driver used logic	EIA RS 422
Max. angular acceleration	$250\,000\,\mathrm{rad\,s^{-1}}$
Output current per channel	-20 – 20 mA
Signal rise time	180 ns
Measurement condition for signal rise time	CL=25pF, RL=2.7kOhm
Signal fall time	40 ns
Measurement condition for signal fall time	CL=25pF, RL=2.7kOhm
Phase shift	90 °e
Phase shift, inaccuracy	45 °e
Index synchronized to AB	Yes
Max. moment of inertia of code wheel	$0.6\,\mathrm{g\,cm^2}$
Operating temperature	$-40\,^{\circ}\mathrm{C}$ to $100\,^{\circ}\mathrm{C}$
Orientation of encoder output to motor flange	-1°

shown in Figure 2.9(a). The specifications are given in Table 2.7. This encoder is chosen for its high resolution, simple design, ease of use and compatibility with the motor.

The other two encoders that are on the either side of the spring are hereafter referred as spring encoders. The spring encoders are chosen for their high resolution, ease of use, ability to lock on to a shaft and be bolted on to a frame.

The encoders are 'E3 incremental Optical Kit Encoder' from US Digital, with part no. E3-500-315-NE-H-M-B and E3-500-787-NE-H-M-B. These two encoders differ only in their diameter, one has 8mm hole and other has 12mm diameter hole for the shaft. The encoders have two channels in which channel A leads channel B for

Table 2.8: Specification of the spring encoder.

Specification	Value
Supply Voltage	Min 4.5 V Typ 5.0 V Max 5.5 V
Supply Current	Min 27 mA Max 33 mA
Output Voltage	Min 0.5 V Max 2 V
Output Current	Min -8 mA Max 8 mA
Output Rise Time	100ns
Output Fall Time	35ns
Operating Temperature	$-40\,^{\circ}\mathrm{C}$ to $100\,^{\circ}\mathrm{C}$
Weight	1.28 oz
Max. Acceleration	250000 rad/sec
Max. Shaft Axial Play	0.010 in
Max. Shaft Eccentricity Plus Radial Play	0.004 in

clockwise shaft rotation. The specifications of the spring encoders are given in 2.8. It is shown in Figure 2.9(b).

The product page of the encoder from US Digital' website states 'The E3 is a high resolution rotary encoder with a rugged glass-filled polymer enclosure, which utilizes either a 5-pin locking or standard connector. This optical incremental encoder is designed to easily mount to and dismount from an existing shaft to provide digital feedback information.'

The assembly of motor, planetary gear and encoder is shown in Figure 2.10.

2.3.7 CAD model of the exoskeleton version 2

The exoskeleton is modeled in SolidWorks software. Figure 2.11 shows the CAD model of the exoskeleton. First the base of the frame is modeled such that all the

(a) Motor Encoder HEDL 5540, 500 CPT.

(b) US Digital E3 Rotary incremental optical encoder.

Figure 2.9: Motor encoder and spring encoder of the exoskeleton version 2.

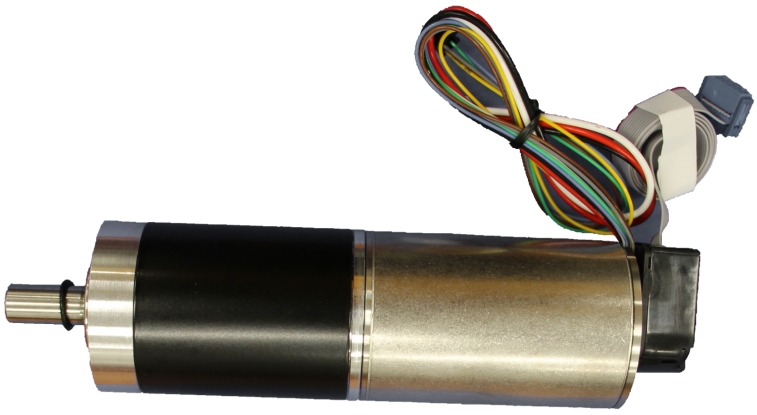

Figure 2.10: Assembly of BLDC motor, planetary gear and motor encoder.

components can be bolted to it. Sheet metal is used to reduce the weight and complexity of the structure while maintaining the strength. It contains a slot to allow any changes in dimensions of the spring. Therefore, a spring of different stiffness can be used in the exoskeleton without modifying the overall design. Also, the components are placed at a distance to the base which allows for different diameters of the motor, gear and spring to be connected.

The motor and planetary gear are factory assembled and they are bolted to the sheet metal holders which are bolted to the base of the frame. Similarly, encoders are bolted to the holders. To hold the motor and planetary gear in place, circular holders are 3D printed. They are made of plastic instead of aluminum since they carry very

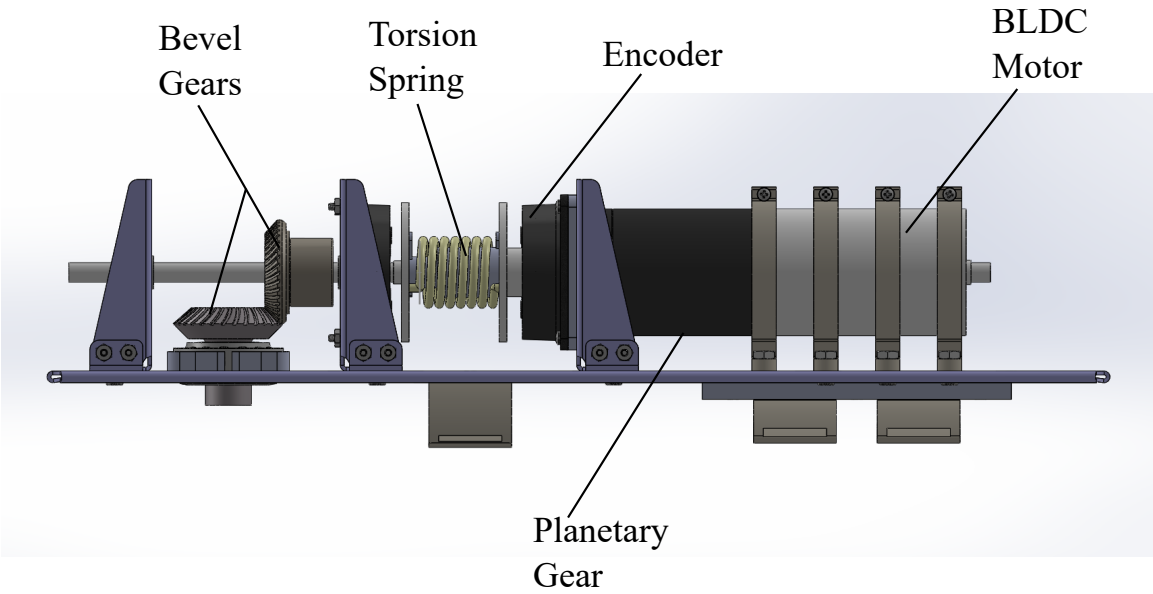

Figure 2.11: CAD model of the exoskeleton version 2.

less load and make the exoskeleton lighter.

The encoders are fixed on the shafts. The shafts sit in the bearing which are fitted in the holders. One of the bevel gears is connected to the shaft and the other bevel gear sits on a tapered roller bearing. It is connected to the lever arm that connects to the shank of the user. The CAD model of the assembly of the frame is shown in Figure 2.12.

The planetary gear shaft is connected to the spring using spring connector. The other end of the spring is connected to other spring connector which has the shaft that holds the bevel gear. The spring connectors have holes that can be used to connect the spring. The diameter of the connector is bigger than the diameter of the spring, so that a different diameter of spring can be used with the same setup. To maintain the spring position, spring mandrels are used. Unlike a single mandrel used in the exoskeleton version 1, exoskeleton version 2 uses two mandrels each connected to spring connectors. These mandrels are of different diameter and concentric to each other with a needle roller bearing sitting between them which help maintain the

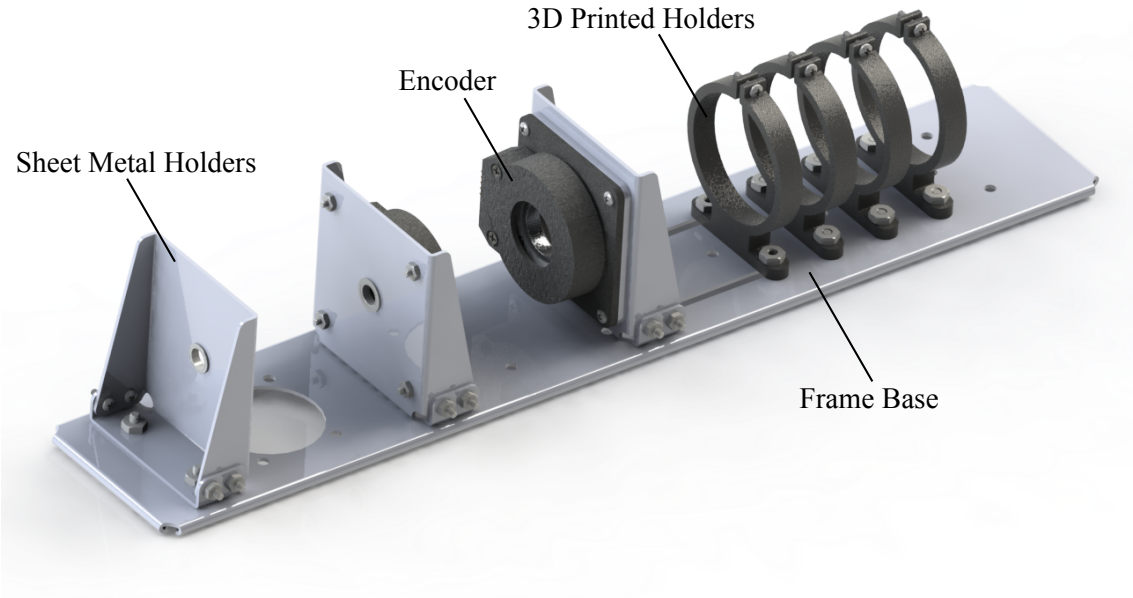

Figure 2.12: CAD model of assembly of frame of exoskeleton version 2.

alignment. The CAD model of assembly of the spring with the connectors is shown in Figure 2.13.

All the parts connect to the base directly using standard bolts 4-40 and 8-32. This makes it easy to assemble. The CAD model of complete assembly of the exoskeleton version 2 is shown in Figure 2.14.

2.3.8 Frame of the exoskeleton version 2

The frame of the exoskeleton is one of the most important part of the exoskeleton. All the components of the exoskeleton are held by the frame. It must be designed to be light in weight for user's comfort, but also rigid enough to support the load of the components. The frame design must also allow for some flexibility for scaling in the future. It should be modular to support any minor modification in spring and other components. It should also be easy to assemble and disassemble.

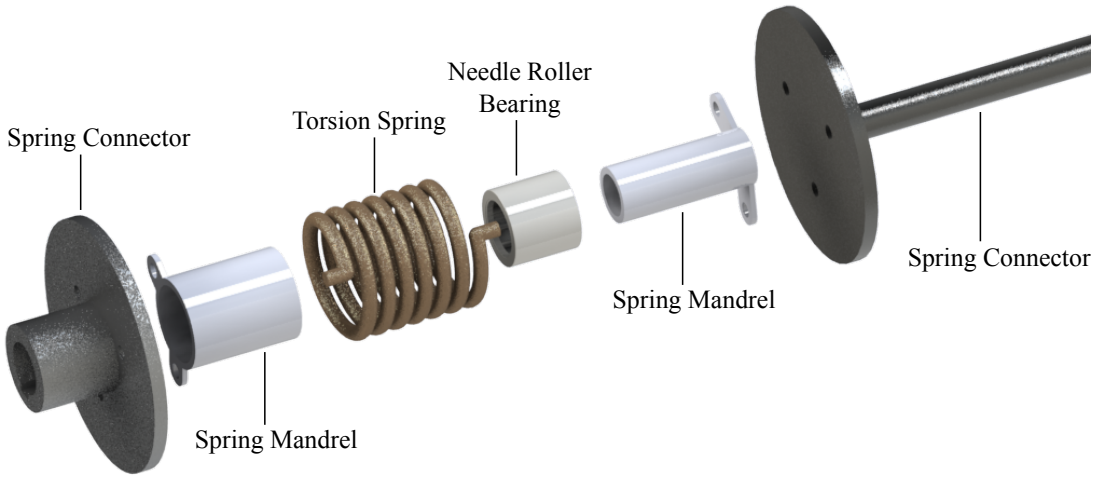

Figure 2.13: CAD model of the spring assembly of exoskeleton version 2.

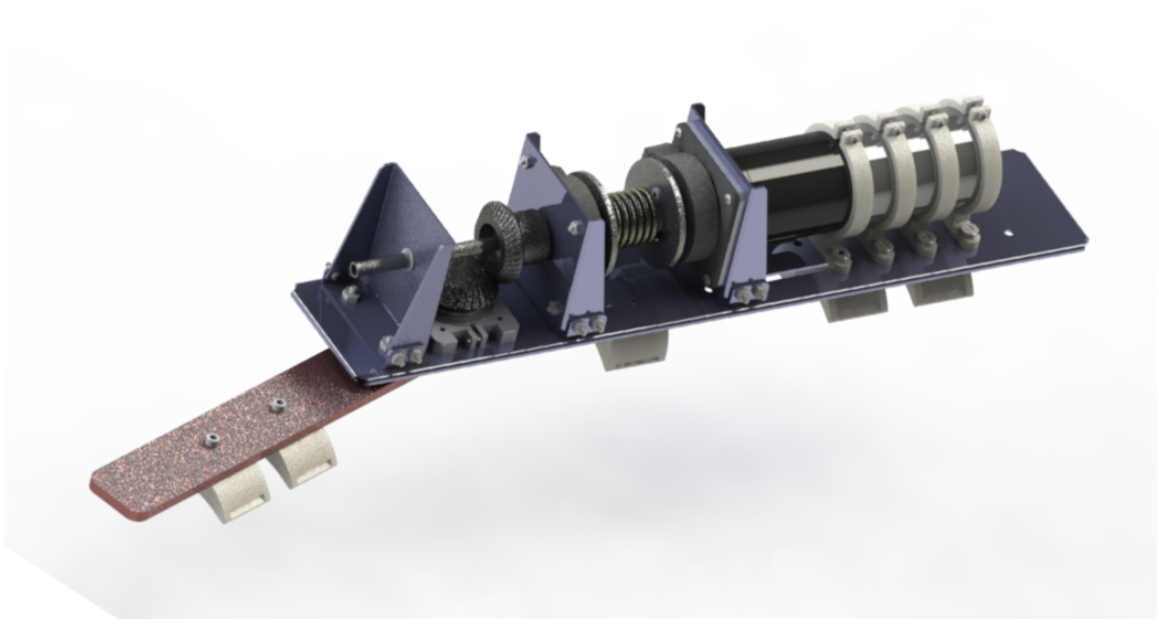

Figure 2.14: CAD model of the complete assembly exoskeleton version 2.

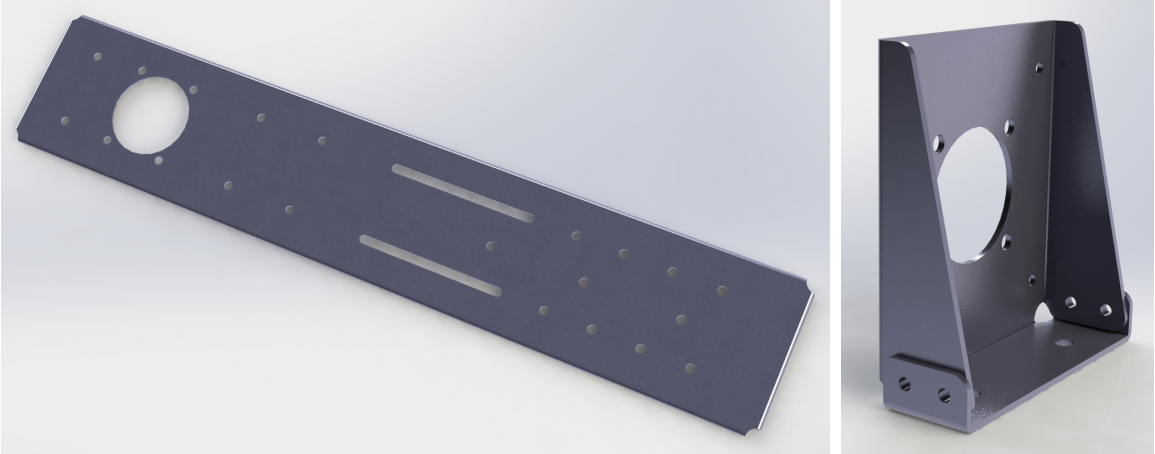

(a) Base of the frame. (b) Sheet metal holders.

Figure 2.15: Base and holders of sheet metal frame.

One of the important factors to consider is the material of the frame. To reduce the overall weight of the exoskeleton, while maintaining the strength and rigidity, aluminum metal is used to fabricate the frame. For the base and connectors, sheet metal 5052 aluminum alloy is used for the frame and 6061 aluminum alloy is used for the parts such as shafts and spring connectors.

The frame is made up of multiple components. The base of the frame is a long sheet metal plate shown in Figure 2.15(a). On this base all the other components are bolted. The motor, spring and the gears are also connected to the frame by sheet metal parts. These parts are bolted perpendicular to the base of the frame. It is shown in Figure 2.15(b).

The sheet metal parts of the frame are waterjet cut and then bent to the required shape. Other parts such as spring connectors, spring mandrel, lever and fillings are machined from aluminum bar stock on lathe and milling machine.

(a) Ball bearing (b) Needle roller bearing (c) Tapered roller bearing

Figure 2.16: Three types of bearings used in the frame of the exoskeleton version 2.

2.3.9 Assembly of the exoskeleton version 2.

Bearings are used for the smooth functioning of the exoskeleton and to support the shaft and the gears. Three types of bearings are used. The needle roller bearing shown in Figure 2.16(b) is used to enable relative motion between the two spring connectors. It is placed between the two spring mandrels and helps to avoid misalignment. To hold the bevel gear in place, a tapered roller bearing is used, shown in Figure 2.16(c). The shaft connecting the spring and bevel gear is held by two roller bearings. It is shown in Figure 2.16(a).

The brace of the exoskeleton is 3D printed as shown in Figure 2.17. Since, each user has a different size of the limb it is custom built for the user of the exoskeleton. This ensures the user is comfortable when using the exoskeleton. It is a minimal design in shape of semi-circle so that the exoskeleton remains compact and lightweight. It can be used with hook-and-loop fasteners to connect to the user's limb.

The complete assembly of the exoskeleton version 2 is shown in Figure 2.18. Figure 2.19 shows the front and side view of exoskeleton version 2 on human leg.

2.3.10 Electronic accessories

The motor driver, controller and battery together form the electronic part of the exoskeleton. For the exoskeleton to be portable and efficient, it is important to have

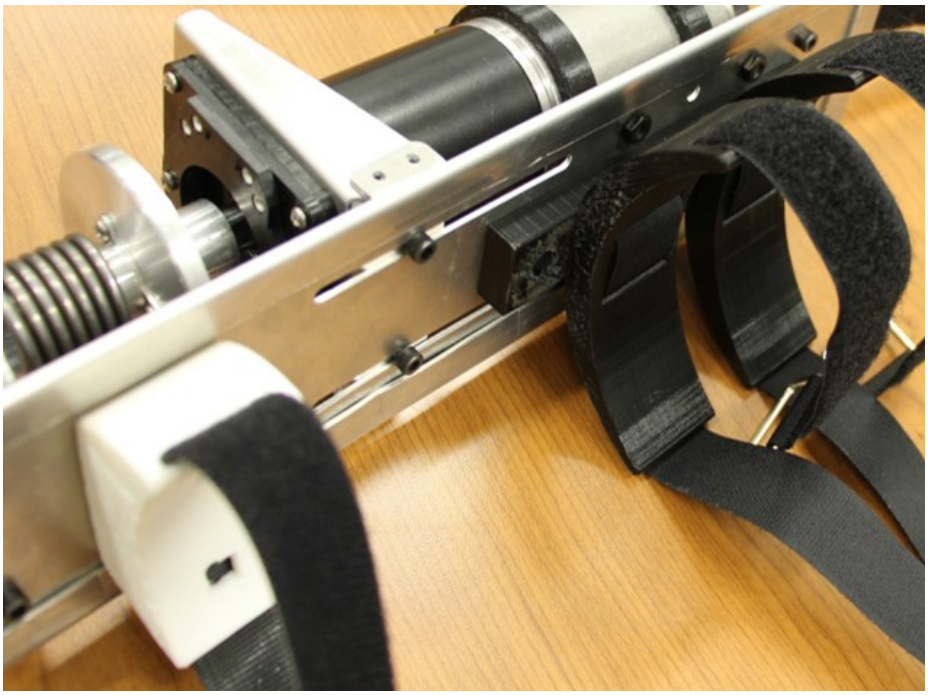

Figure 2.17: 3D printed brace of the exoskeleton version 2.

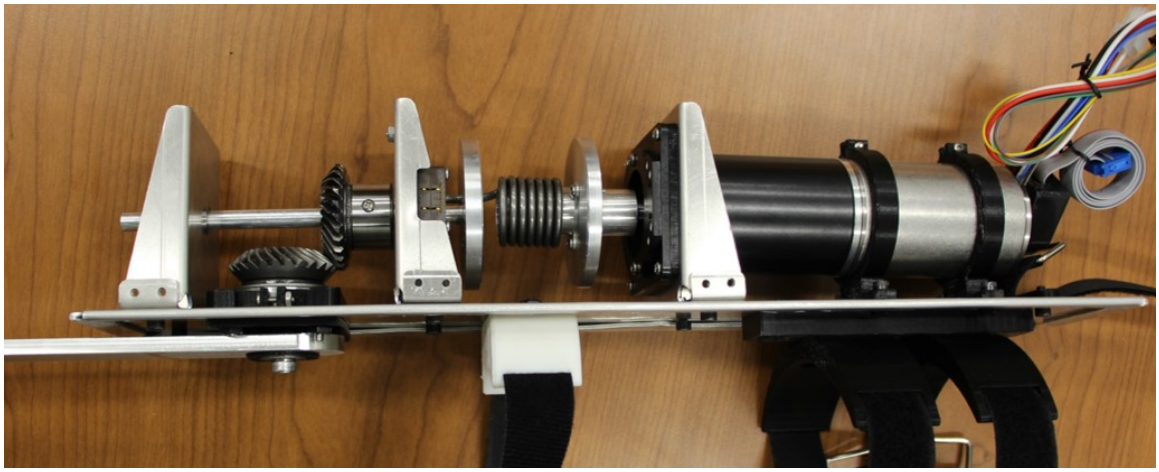

Figure 2.18: Complete assembly of the exoskeleton version 2.

(a) Front view of the exoskeleton

(b) Side view of the exoskeleton

Figure 2.19: The front and side view of exoskeleton version 2 on human leg.

good selection of electronics.

Motor driver

The motor driver powers and controls the motor. It receives position feedback from the motor encoder and powers the motor with corresponding voltage for the motor to reach the desired position and velocity. It can also receive control signals from the real-time controller.

The motor driver is responsible for keeping the motor safe from incidents such as short circuit, over voltage, over speeding, etc. It must have good inbuilt tools to generate signals and should be programmable. It should be able to drive different motors. It should also be compact and lightweight.

Table 2.9: Specification of the motor driver AMC DZRALTE-020L080.

Specification	Value
Size (mm)	63.5 x 50.8 x 22.9
Weight	105 g
Rated Power Continuous	0.9 kW
Rated Power Peak	1.5 kW
Current Continuous	12.0 A
Current Peak	20.0 A
DC Supply Voltage	10 – 80 VDC
Network Communication	Modbus RTU, RS-485/232

The motor driver 'DZRALTE-020L080' from Advanced Motion Controls is selected as it satisfies all the above mentioned requirements. It is shown in Figure 2.20 and the specification are listed in Table 2.9.

Controller

The controller is used to run control algorithms to calculate the optimum assistive torque and the speed of the exoskeleton. It sends control signals to the motor driver such as the desired position and speed. It also receives position feedback from the encoders present in the exoskeleton.

The controller should be a very fast and should operate in real-time. It should be compact to make the exoskeleton portable. It should have multiple I/O pins to connect to encoders and drivers.

MyRIO-1900 from National Instruments is a suitable controller for this purpose. It is an embedded controller with a real-time processor. It has a dual-core ARM microprocessor and a Xilinx FPGA. LabVIEW, a visual programming software is used to program myRIO. Figure 2.20 shows the image of myRIO.

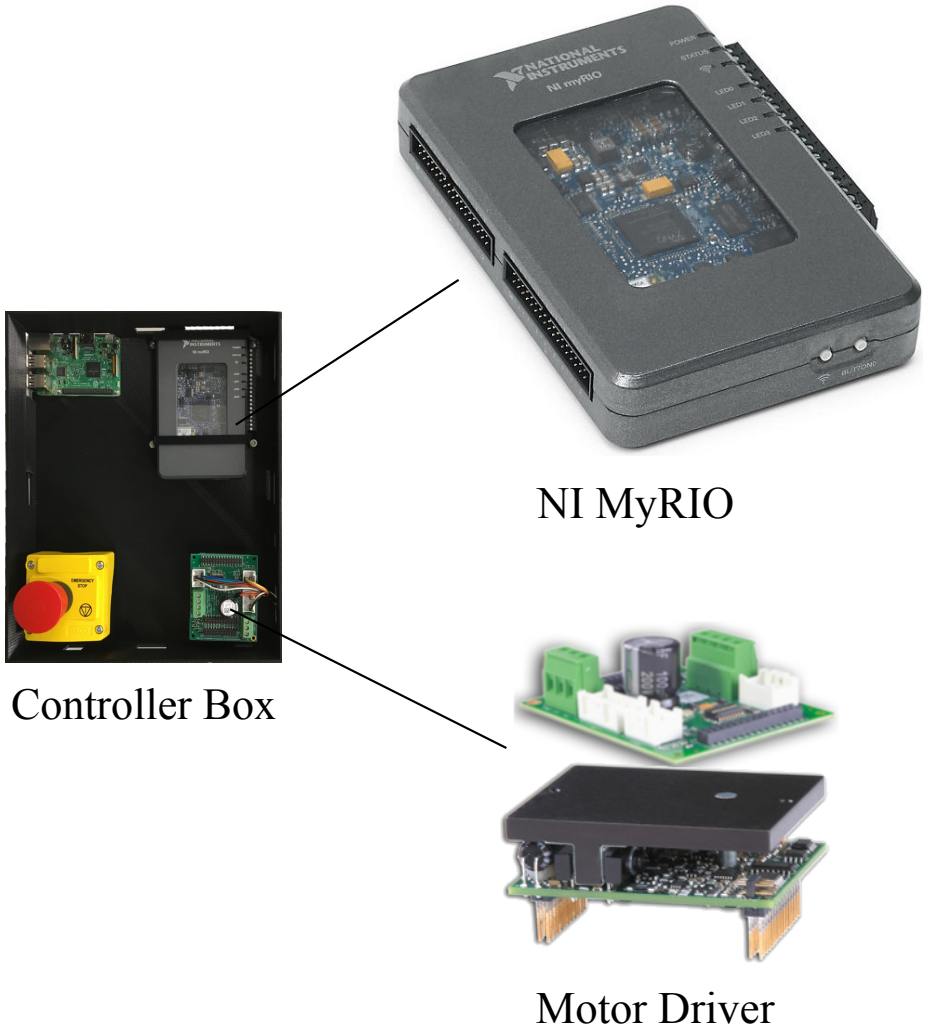

Figure 2.20: Controller setup for the exoskeleton version 2.

Battery

The motor works on a 24 V power supply regulated from the motor driver. This power can be sourced from an external power supply box or a portable battery. A portable power supply provides mobility to the user which amplifies the benefits of the exoskeleton. A 36V Lithium-Ion 2.0 Ah SlimPack Battery from Bosch shown in Figure 2.21 is selected as the power supply for the exoskeleton. It has higher voltage than the motor, which is regulated by the motor driver to correct any fluctuations in the power. The same battery with the motor driver can power a variety of different

Figure 2.21: 36 V 2.0 Ah Li-ion battery.

motors. It weighs 700 g. The only drawback with using a battery source is that the it lasts for a limited time and needs to be charged before it is used again. It should however be good for a 20-minute training session.

2.4 Chapter summary

In this chapter the features of the first version of the exoskeleton are studied with emphasis on its problems and limitations. The motivation for a new version of exoskeleton is presented and a new design of the exoskeleton is proposed. The design requirements and biomechanical design considerations are presented. The components of the exoskeleton such as motor, gear, spring, encoders, driver and controller and their selection process are explored in detail. The CAD model, the design choices and the assembly of the second version of the exoskeleton are detailed.

Chapter 3

CONTROL AND TESTING OF THE EXOSKELETON

3.1 Control of the exoskeleton

The exoskeleton can be controlled to provide assistive torque to the human knee for different gait phases and activities. A controller is used to generate the desired torque and a motor driver is used to control the motor based on the desired torque. The exoskeleton can be used along with inertial measurement units (IMU) and other sensors that can measure and detect various gait parameters (Chinmilli *et al.* (2017)). Using motion capture and markers, lower body joint angular displacements and gait parameters such as cadence and step length are computed. The knee joint moment can be estimated by applying inverse dynamics to the multi-body model given in (Ramakrishnan *et al.* (1991)).

There are two ways to provide the desired knee assistive torque. The first approach is by using reference knee trajectory for the gait cycle (Unluhisarcikli *et al.* (2011)). In this approach a knee trajectory of a healthy person is used as a reference for the control of the exoskeleton. This is used to generate the respective desired torque for the knee angle in the gait cycle.

Another approach is to provide setpoint knee angle conditions for different gait phases (Ranzani (2014)). In this approach, setpoints are defined for every gait phase separately. The gait phases and activities can be detected using IMUs and smart shoes (Chinimilli *et al.* (2017)). The impedance parameters such as actuator stiffness and damping can be provided using AIT algorithm (Chinimilli *et al.* (2018)). These parameters are then used to calculate the desired assistive torque.

The desired knee assistive torque to be exerted on the human by the exoskeleton can be defined as:

$$T_d(t) = K(\theta_{SP} - \theta_H(t)) + B\dot{\theta}_H(t) \tag{3.1}$$

where T_d is the desired torque. K, B and θ_{SP} are the actuator stiffness, damping, and set point angle respectively, given by smart shoe and IMUs, and θ_H is the human-side angle.

Since the exoskeleton is a series elastic actuator, the generated torque is proportional to the motor position (Kong *et al.* (2012)), i.e., the desired torque can be achieved by controlling the motor position. After calculating the torque reference, the reference position of the motor is calculated and the motor tracks the reference position using a cascaded PID (proportional-integral-derivative) control loop, in which the inner loop controls the motor velocity and the outer loop controls the position.

$$T = K_s(\theta_{M*} - \theta_{H*})N_s \tag{3.2}$$

$$\theta_{H*} = \theta_H/N_S \tag{3.3}$$

$$\theta_{M*} = \theta_M N_W \tag{3.4}$$

where T is the torque provided by the exoskeleton, θ_M is the motor angle, N_s is the spur gear ratio and N_W is the worm gear ratio, θ_{M*} is worm gear angle and θ_{H*} is spur gear angle for the first version of exoskeleton. In the second version of exoskeleton similar control algorithm can be used. Where the worm gear ratio is replaced by planetary gear ratio and spur gear ratio is replaced by bevel gear ratio.

This control algorithm can be implemented in a controller setup. As described

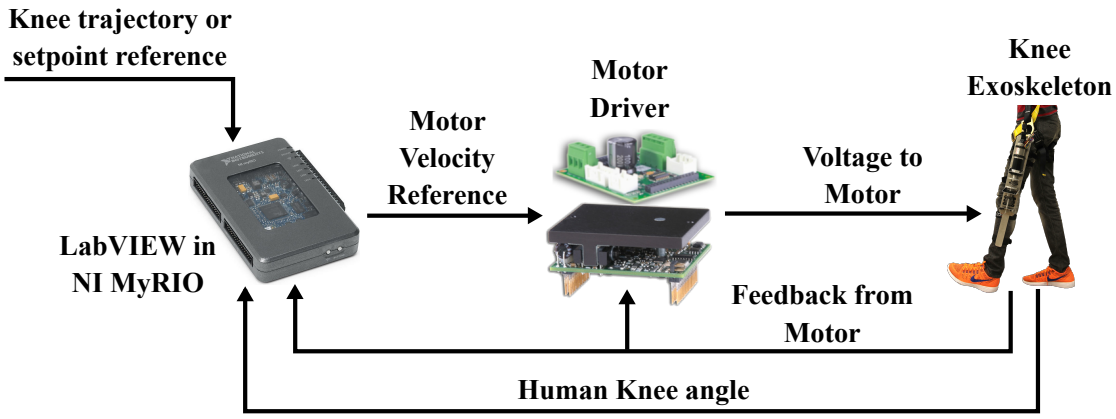

Figure 3.1: The control block diagram for the knee exoskeleton.

in Chapter 2, the NI MyRIO controller can be used with AMC DZRALTE-020L080 motor driver to control the exoskeleton. The MyRIO can be programmed using LabVIEW. Smart shoes measure ground contact forces, along with IMUs measurement, are used to provide real-time activity recognition and gait phase detection. The impedance parameters such as K, B and setpoint angle from the IMUs and smart shoes are input to the MyRIO. It also receives human knee angle and motor feedback from the exoskeleton. Based on the desired torque, the velocity reference for the motor is calculated by the MyRIO and sent to the motor driver as input. The motor driver uses a cascaded PID control loop to control the velocity of the motor. The control block diagram for the knee exoskeleton is presented in Figure 3.1.

Using the AIT algorithm, experiments were conducted with the first version of exoskeleton with NI cRIO as controller. It has been shown that the knee exoskeleton was able to reduce the RMS value of EMG signal of Vastus Medialis of two subjects (Chinimilli *et al.* (2018)). By providing assistive torque in the stance phase, the corresponding muscle activity was reduced. The walking experiment setup is shown

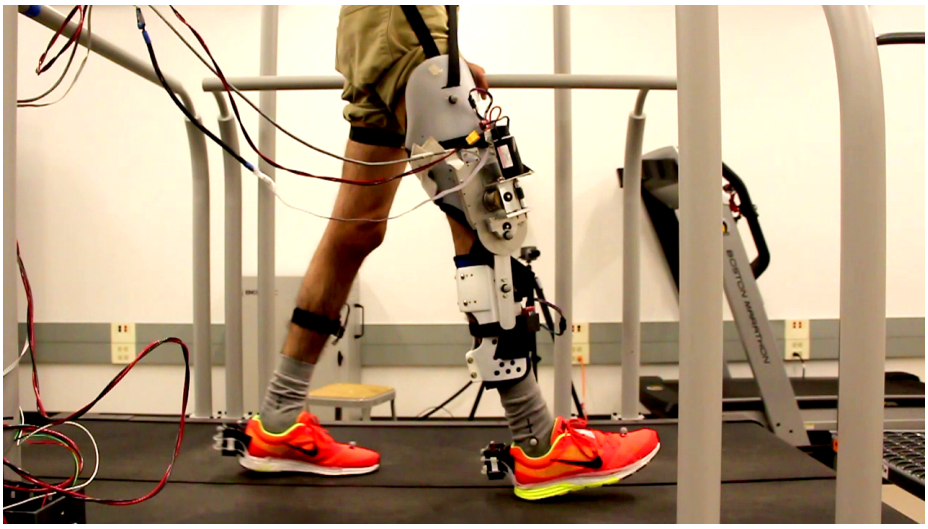

Figure 3.2: Walking experiment with the exoskeleton version 1 on the treadmill.

in the Figure 3.2.

It was observed during the experiment that the torque output could be higher for better assistance. Also, when the exoskeleton is worn for a long period of time and it becomes uncomfortable to use. The new exoskeleton solves these problems and therefore should yield better results in similar experiments.

3.2 Testing of the exoskeleton version 2

Before the exoskeleton is used in an experiment, it must be tested. First, bench testing needs to be done to make sure the exoskeleton is able to track the reference signal. Later walking experiment will be done to gauge the effectiveness of the exoskeleton version 2.

The first bench test is to drive the motor using motor driver and measure the values from the motor encoder and spring encoders. A sinusoidal signal can be used as reference. Comparing the encoder values with the reference signal will show the performance of the motor control. The motor uses a PID control loop to track the signal. The gains of the PID control can be varied to improve the performance of the

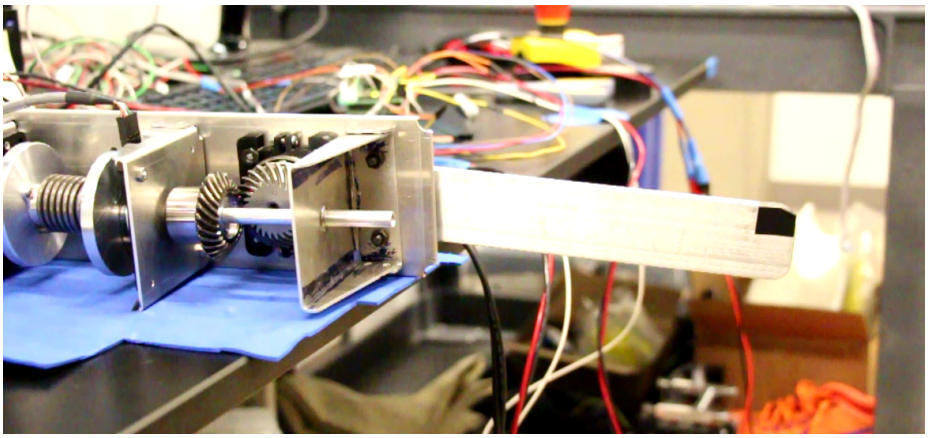

Figure 3.3: Bench testing of the exoskeleton version 2.

system. The bench testing setup is shown in figure 3.3.

In the second test, the signal is generated from the controller. A periodic reference knee trajectory is generated from the MyRIO, which is sent to the motor driver. Again the encoder values are compared with the reference signal. A control loop can be implemented in the controller to improve the performance of the trajectory following.

These tests are used to measure the performance of the motor, driver and controller. To measure the performance of the encoder, another control algorithm can be implemented that uses feedback from encoder as reference for the motor to follow.

Once the exoskeleton shows satisfactory performance in the bench tests, it can be worn by the subject in a walking test and different torque assistance algorithm can be implemented.

3.3 Chapter summary

In this chapter, the impedance-based control algorithm and its implementation in the control setup for the first and second version of exoskeleton is presented. The bench testing of the exoskeleton version 2 is detailed.

Chapter 4

DISCUSSION

4.1 Comparison

A comparison of version 1 and version 2 of exoskeleton is presented in Table 4.1. It can be seen that the exoskeleton version 2 is designed according to design requirements and it is an improvement over the version 1. The maximum torque output and torque to weight ratio is increased with only small increase in weight.

Table 4.1: A comparison of exoskeleton version 1 and version 2.

	Version 2	Version 1
Total Reduction ratio	53:1	63.6:1
Maximum continuous torque output	23 N·m	11.2 N·m
Maximum continuous speed	79.62 rpm	120 rpm
Total weight	2.83 kg	2.4 kg
Total size	17 x 4.5 x 3.5 in	9 x 4.5 x 4.5 in
Torque to weight ratio	8.13 N·m/kg	4.67 N·m/kg

A comparison of exoskeleton version 2 with the state of the art designs is done in Table 4.2. The list of the exoskeletons mentioned in the table is given below.

1. Exoskeleton version 2
2. cRSEA (Kong *et al.* (2012))
3. Torque dense exoskeleton (Zhu *et al.* (2017))
4. Indego (Martínez *et al.* (2017); Murray *et al.* (2015))
5. Modular lower limb exoskeleton (Bartenbach *et al.* (2016))
6. Four-bar linkage exoskeleton (Kim *et al.* (2015))

Table 4.2: Comparison of the new version of exoskeleton with the state of the art.

	Max continuous torque output (N·m)	Max continuous speed (rpm)	Total weight (kg)	Torque to weight ratio (N·m/kg)	Mechanism
1	23	79.62	2.83	8.13	BLDC motor, planetary gear and bevel gear
2	10.86	140	–	–	DC motor, worm gear and spur gear
3	30	80	4.88	6.14	PMSM, planetary gear and timing belt
4	20	–	12	1.66	BLDC motor and 24:1 gear reduction
5	80	30	25	3.2	BLDC motor and 160:1 ratio harmonic drive
6	42.9	37.55	3.5	12.25	DC motor, 100:1 harmonic drive and four-bar linkage

4.2 Discussion

A proposed design of exoskeleton is fabricated according to the design requirements. The following are the areas where the design is improved.

The brace in the version 1 design is heavy (0.83 kg), bulky, and difficult to wear. By reducing the weight of the brace, overall weight of the exoskeleton is reduced. In version 2, a simple brace is designed and 3D printed to fasten the exoskeleton to the human leg. It is lightweight, compact and easy to wear which is a considerable improvement over the version 1.

In the version 1 design, the axis of rotation changes twice, which might cause alignment issues. The design of version 2 has only one change in axis, hence preventing any alignment issues with prolonged usage. Multiple encoders are used in exoskeleton version 2 and they are placed close to the spring to accurately track the deflection of the spring and measure the torque. It helps to address the problem of backlash and inaccuracy.

The new exoskeleton has a higher torque to weight ratio of 8.13 N·m/kg. Hence, it could help in improving the rehabilitation training process.

The frame of the exoskeleton is designed to be modular and customizable. This helps in scaling and modifying the exoskeleton to the needs and demands of the patient and stay on par with the changes in the technology.

4.3 Chapter summary

In this chapter, a comparison of first and second version of exoskeleton is presented. Also, the exoskeleton version 2 is compared with the state of the art designs. A discussion is also presented.

Chapter 5

CONCLUSION AND FUTURE WORK

5.1 Summary and conclusion

An overview of the exoskeleton is presented along with details of the lower-limb exoskeletons and knee exoskeletons. A detailed analysis of the first version of exoskeleton is done. Using the limitations of the first version as motivation, a new exoskeleton design is proposed.

The exoskeleton version 2 is developed by defining design requirements and biomechanical considerations and selecting the components based on those requirements. A 180 W BLDC motor is selected as the actuator. A planetary gear with 53:1 gear ratio connected to the motor is used to amplify the torque to the required amount of assistance. The direction of the transmission is changed using 1:1 ratio bevel gear. A torsion spring is used to connect the planetary gear and bevel gear and acts as a torque sensor in the control design. It makes the exoskeleton a series elastic actuator.

A frame is built using 5052 sheet metal aluminum alloy. This frame holds the components of the exoskeleton. It is modeled to be modular and easy to assemble. A minimal 3D printed brace is used in the exoskeleton version 2. The controller setup including a controller, motor driver and battery is used to control the exoskeleton.

The control logic and implementation are shown and bench tests are explored. A comparison is made between the first and second version of exoskeleton. Also, exoskeleton version 2 and the state of the art devices are compared. The version 2 is designed to overcome the problems of the version 1. However, further testing needs to be done, to prove its effectiveness. The future work is presented in the next section.

5.2 Future work

Although the exoskeleton version 2 is an improvement over the version 1, there are areas where it can be improved. Some of these corresponds to the components used in the exoskeleton, some are related to the mechanical structure and some are indirectly related to the exoskeleton such as controller box, etc.

The first major problem to the user could be the length of the exoskeleton. It is 17 inches long, which could be problem for people who are shorter. It may affect their walking pattern. Therefore, reducing the size of the exoskeleton should be prioritized. This could be done by using a motor and gear with smaller length and changing the placement of bevel gear.

The motor and planetary gear are held to the frame by one holder. Only other support are the 3D printed holders. This could be a problem because the holders are bolted to the frame and may not sustain unexpected heavy loads. Therefore, a better supporting mechanism needs to be designed to hold the motor and planetary gear.

To maintain the compactness of the exoskeleton, a small ratio of the bevel gear is used. This choice resulted in the increase in the planetary gear ratio. Due to this, the weight of the planetary gear is increased. Therefore, a higher ratio bevel gear needs to be used which is still compact enough to fit in the exoskeleton.

The bevel gear connecting to the lever arm sits inside the tapered roller bearing, which is fixed to the base of the frame. This may cause issues with alignment. A better holding structure needs to be designed that can secure the tapered bearing to the frame.

The bevel gear is connected to the shaft with a threaded bolt. This may not be desirable when using the exoskeleton for high torque output, or when impact loading is expected. Additional method for securing the bevel gear to the shaft such as using

a key between bevel gear and shaft needs to be explored.

The safety of the user should be considered high priority. Therefore, limits must be put in place so that the user can be prevented from accidents. Multiple mechanical, electronic and software limits must be put in place. Some of which include use of emergency stop button, mechanical limits on the lever arm and using safety conditions in the program.

Although the brace of the exoskeleton is designed to be lightweight and easy to wear, the connection of brace to the exoskeleton may not be very secure. A design should be implemented which integrates the brace to the frame of the exoskeleton.

The controller setup can be improved so that all the electronics are integrated. It could also be made portable so that it can be placed on the waist or the back of the user. Some of the design improvements could be use of custom printed circuit board to eliminate or reduce the use of wires and use of integrated controller and motor driver.

To reduce the weight of the exoskeleton on the limb of the user, it is supported using a shoulder harness, which makes the shoulder to bear some of the weight of the exoskeleton. A custom harness could be designed which has harness on the waist so that some of the weight would be transferred to the waist.

Before the exoskeleton can be worn the user, the exoskeleton will be tested for its functionality and effectiveness. To begin with, the following bench tests will be done on the exoskeleton. In the first test the performance of tracking the sinusoidal signal that is commanded from the motor driver is evaluated. In the second test, tracking of the reference signal that is commanded from the controller is examined. In the third test, the motor is programmed to follow the lever arm motion using the feedback from the encoder. In the final bench test, the ability of the exoskeleton to reject external disturbances from the environment studied.

After the bench tests are done, the walking test with the exoskeleton will be done on the healthy subjects. The tests can be varied using instrumented treadmill to change the walking speeds and inclination angle. The exoskeleton will be used by subjects that vary in height and weight, to measure the effect of similar assistance on different subjects. Implementation of different control algorithm will be done using the exoskeleton. The exoskeleton can also be integrated with other assistive devices such as ankle exoskeleton and wearable sensors such as smart shoes and IMUs that measure ground contact forces and detect gait phases and activities. Various gait metrics will be recorded and studied such as cadence, range of motion, EMG values, etc.

Once the tests are done, the exoskeleton can be used by patients in their rehabilitation training.

REFERENCES

Banala, S. K., S. H. Kim, S. K. Agrawal and J. P. Scholz, "Robot assisted gait training with active leg exoskeleton (alex)", IEEE transactions on neural systems and rehabilitation engineering **17**, 1, 2–8 (2009).

Bartenbach, V., M. Gort and R. Riener, "Concept and design of a modular lower limb exoskeleton", in "Biomedical Robotics and Biomechatronics (BioRob), 2016 6th IEEE International Conference on", pp. 649–654 (IEEE, 2016).

Bolivar, E., D. Allen, G. Ellson, J. Cossio, W. Voit and R. Gregg, "Towards a series elastic actuator with electrically modulated stiffness for powered ankle-foot orthoses", in "Automation Science and Engineering (CASE), 2016 IEEE International Conference on", pp. 1086–1093 (IEEE, 2016).

Celebi, B., M. Yalcin and V. Patoglu, "Assiston-knee: A self-aligning knee exoskeleton", in "Intelligent Robots and Systems (IROS), 2013 IEEE/RSJ International Conference on", pp. 996–1002 (IEEE, 2013).

Cenciarini, M. and A. M. Dollar, "Biomechanical considerations in the design of lower limb exoskeletons", in "Rehabilitation Robotics (ICORR), 2011 IEEE International Conference on", pp. 1–6 (IEEE, 2011).

Chinimilli, P. T., Z. Qiao, S. M. R. Sorkhabadi, V. Jhawar, I. H. Fong and W. Zhang, "Automatic virtual impedance adaptation of a knee exoskeleton for personalized walking assistance (submitted)", (2018).

Chinimilli, P. T., S. Redkar and W. Zhang, "Human activity recognition using inertial measurement units and smart shoes", in "American Control Conference (ACC), 2017", pp. 1462–1467 (IEEE, 2017).

Chinimilli, P. T., S. W. Wachtel, P. Polygerinos and W. Zhang, "Hysteresis compensation for ground contact force measurement with shoe-embedded air pressure sensors", in "ASME 2016 Dynamic Systems and Control Conference", pp. V001T09A006–V001T09A006 (American Society of Mechanical Engineers, 2016).

Chinmilli, P., S. Redkar, W. Zhang and T. Sugar, "A review on wearable inertial tracking based human gait analysis and control strategies of lower-limb exoskeletons", Int Rob Auto J **3**, 7, 00080 (2017).

Colombo, G., M. Joerg, R. Schreier, V. Dietz *et al.*, "Treadmill training of paraplegic patients using a robotic orthosis", Journal of rehabilitation research and development **37**, 6, 693–700 (2000).

Dollar, A. M. and H. Herr, "Design of a quasi-passive knee exoskeleton to assist running", in "Intelligent Robots and Systems, 2008. IROS 2008. IEEE/RSJ International Conference on", pp. 747–754 (IEEE, 2008a).

Dollar, A. M. and H. Herr, "Lower extremity exoskeletons and active orthoses: challenges and state-of-the-art", IEEE Transactions on robotics **24**, 1, 144–158 (2008b).

Fick, B. R. and J. B. Makinson, "Hardiman I prototype for machine augmentation of human strength and endurance", Tech. rep., GE Co. Schenectady, NY. (1971).

Gage, H. and L. Storey, "Rehabilitation for parkinson's disease: a systematic review of available evidence", Clinical rehabilitation **18**, 5, 463–482 (2004).

Gilbert, K. E. and P. C. Callan, "HARDIMAN I PROTOTYPE PROJECT", Tech. rep., GE Co. Schenectady, NY. (1968).

Grosu, V., C. Rodriguez Guerrero, S. Grosu, B. Vanderborght and D. Lefeber, "Design of smart modular variable stiffness actuators for robotic assistive devices", IEEE/ASME Trans. Mechatron p. 1 (2017).

He, W., D. Goodkind, P. Kowal *et al.*, "An aging world: 2015. international population reports, p95/16-1", (2016).

Herr, H., "Exoskeletons and orthoses: classification, design challenges and future directions", Journal of neuroengineering and rehabilitation **6**, 1, 21 (2009).

Kawamoto, H., S. Lee, S. Kanbe and Y. Sankai, "Power assist method for hal-3 using emg-based feedback controller", in "Systems, Man and Cybernetics, 2003. IEEE International Conference on", vol. 2, pp. 1648–1653 (IEEE, 2003).

Kawamoto, H. and Y. Sankai, "Power assist system hal-3 for gait disorder person", in "International Conference on Computers for Handicapped Persons", pp. 196–203 (Springer, 2002).

Kazerooni, H. and R. Steger, "The berkeley lower extremity exoskeleton", Journal of dynamic systems, measurement, and control **128**, 1, 14–25 (2006).

Kim, J.-H., M. Shim, D. H. Ahn, B. J. Son, S.-Y. Kim, D. Y. Kim, Y. S. Baek and B.-K. Cho, "Design of a knee exoskeleton using foot pressure and knee torque sensors", International Journal of Advanced Robotic Systems **12**, 8, 112 (2015).

Kim, S. and J. Bae, "Force-mode control of rotary series elastic actuators in a lower extremity exoskeleton using model-inverse time delay control", IEEE/ASME Transactions on Mechatronics **22**, 3, 1392–1400 (2017).

Kong, K., J. Bae and M. Tomizuka, "A compact rotary series elastic actuator for human assistive systems", IEEE/ASME transactions on mechatronics **17**, 2, 288–297 (2012).

Lockheed Martin, "Fortis - exoskeleton technologies: Industrial", `https://lockheedmartin.com/en-us/products/exoskeleton-technologies/industrial.html`, [Online; accessed 2-July-2018] (2018).

Martínez, A., B. Lawson and M. Goldfarb, "Preliminary assessment of a lower-limb exoskeleton controller for guiding leg movement in overground walking", in "Rehabilitation Robotics (ICORR), 2017 International Conference on", pp. 375–380 (IEEE, 2017).

Mosher, R. S., "Handyman to hardiman", Sae Transactions pp. 588–597 (1968).

Murray, S. A., K. H. Ha, C. Hartigan and M. Goldfarb, "An assistive control approach for a lower-limb exoskeleton to facilitate recovery of walking following stroke", IEEE Transactions on Neural Systems and Rehabilitation Engineering **23**, 3, 441–449 (2015).

Ortman, J. M., V. A. Velkoff, H. Hogan *et al.*, *An aging nation: the older population in the United States* (United States Census Bureau, Economics and Statistics Administration, US Department of Commerce, 2014).

Park, Y.-L., J. Santos, K. G. Galloway, E. C. Goldfield and R. J. Wood, "A soft wearable robotic device for active knee motions using flat pneumatic artificial muscles", in "Robotics and Automation (ICRA), 2014 IEEE International Conference on", pp. 4805–4810 (IEEE, 2014).

Polygerinos, P., N. Correll, S. A. Morin, B. Mosadegh, C. D. Onal, K. Petersen, M. Cianchetti, M. T. Tolley and R. F. Shepherd, "Soft robotics: Review of fluid-driven intrinsically soft devices; manufacturing, sensing, control, and applications in human-robot interaction", Advanced Engineering Materials (2017).

Pransky, J., "The pransky interview: Russ angold, co-founder and president of ekso labs", Industrial Robot: An International Journal **41**, 4, 329–334 (2014).

Pratt, G. A. and M. M. Williamson, "Series elastic actuators", in "Intelligent Robots and Systems 95.'Human Robot Interaction and Cooperative Robots', Proceedings. 1995 IEEE/RSJ International Conference on", vol. 1, pp. 399–406 (IEEE, 1995).

Pratt, J. E., B. T. Krupp, C. J. Morse and S. H. Collins, "The roboknee: an exoskeleton for enhancing strength and endurance during walking", in "Robotics and Automation, 2004. Proceedings. ICRA'04. 2004 IEEE International Conference on", vol. 3, pp. 2430–2435 (IEEE, 2004).

Ramakrishnan, H., G. Masiello and M. Kadaba, "On the estimation of the three dimensional joint moments in gait", in "ASME Biomechanics Symposium", vol. 120, pp. 333–339 (1991).

Ranzani, R., *Adaptive human model-based control for active knee prosthetics*, Master's thesis, ETH Zürich (2014).

Robinson, D. W., *Design and analysis of series elasticity in closed-loop actuator force control*, Ph.D. thesis, Massachusetts Institute of Technology (2000).

Shamaei, K., M. Cenciarini, A. A. Adams, K. N. Gregorczyk, J. M. Schiffman and A. M. Dollar, "Biomechanical effects of stiffness in parallel with the knee joint during walking", IEEE Transactions on Biomedical Engineering **62**, 10, 2389–2401 (2015).

Shamaei, K. and A. M. Dollar, "On the mechanics of the knee during the stance phase of the gait", in "Rehabilitation Robotics (ICORR), 2011 IEEE International Conference on", pp. 1–7 (IEEE, 2011).

Shepherd, M. and E. Rouse, "Design and validation of a torque-controllable knee exoskeleton for sit-to-stand assistance", IEEE ASME Trans. Mechatron pp. 1–1 (2017).

Sridar, S., Z. Qiao, N. Muthukrishnan, W. Zhang and P. P. Polygerinos, "A soft-inflatable exosuit for knee rehabilitation: Assisting swing phase during walking", Frontiers in Robotics and AI **5**, 44 (2018).

UNFPA, "Ageing in the twenty-first century: A celebration and a challenge", `https://www.unfpa.org/publications/ageing-twenty-first-century`, [Online; accessed 16-July-2018] (2012).

Unluhisarcikli, O., M. Pietrusinski, B. Weinberg, P. Bonato and C. Mavroidis, "Design and control of a robotic lower extremity exoskeleton for gait rehabilitation", in "Intelligent Robots and Systems (IROS), 2011 IEEE/RSJ International Conference on", pp. 4893–4898 (IEEE, 2011).

Veneman, J. F., R. Kruidhof, E. E. Hekman, R. Ekkelenkamp, E. H. Van Asseldonk and H. Van Der Kooij, "Design and evaluation of the lopes exoskeleton robot for interactive gait rehabilitation", IEEE Transactions on Neural Systems and Rehabilitation Engineering **15**, 3, 379–386 (2007).

Weinberg, B., J. Nikitczuk, S. Patel, B. Patritti, C. Mavroidis, P. Bonato and P. Canavan, "Design, control and human testing of an active knee rehabilitation orthotic device.", in "ICRA", pp. 4126–4133 (Citeseer, 2007).

Winter, D. A., *Biomechanics and motor control of human gait: normal, elderly and pathological* (University of Waterloo Press, 1991).

Wolf, S., G. Grioli, O. Eiberger, W. Friedl, M. Grebenstein, H. Höppner, E. Burdet, D. G. Caldwell, R. Carloni, M. G. Catalano *et al.*, "Variable stiffness actuators: Review on design and components", IEEE/ASME transactions on mechatronics **21**, 5, 2418–2430 (2016).

Yagn, N., "Apparatus for facilitating walking", U.S. Patent 420,179, 28 Jan., (1890).

Yakimovich, T., J. Kofman and E. D. Lemaire, "Design and evaluation of a stance-control knee-ankle-foot orthosis knee joint", IEEE Transactions on neural systems and rehabilitation engineering **14**, 3, 361–369 (2006).

Zhang, W., M. Tomizuka and N. Byl, "A wireless human motion monitoring system for smart rehabilitation", Journal of Dynamic Systems, Measurement, and Control **138**, 11, 111004 (2016).

Zhu, H., J. Doan, C. Stence, G. Lv, T. Elery and R. Gregg, "Design and validation of a torque dense, highly backdrivable powered knee-ankle orthosis", in "Robotics and Automation (ICRA), 2017 IEEE International Conference on", pp. 504–510 (IEEE, 2017).

Zhu, Y., J. Yang, H. Jin, X. Zang and J. Zhao, "Design and evaluation of a parallel-series elastic actuator for lower limb exoskeletons", in "Robotics and Automation (ICRA), 2014 IEEE International Conference on", pp. 1335–1340 (IEEE, 2014).